



## Review

# Recent development of ceria-based (nano)composite materials for low temperature ceramic fuel cells and electrolyte-free fuel cells

Liangdong Fan <sup>a,b</sup>, Chengyang Wang <sup>b,\*,</sup> Mingming Chen <sup>b</sup>, Bin Zhu <sup>a,b,\*</sup>

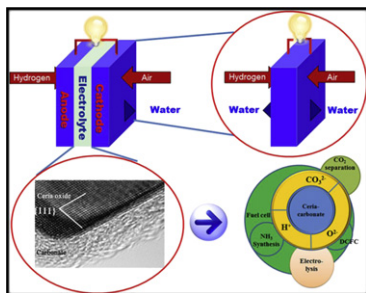
<sup>a</sup> Department of Energy Technology, Royal Institute of Technology (KTH), S-10044 Stockholm, Sweden

<sup>b</sup> Key Laboratory for Green Chemical Technology of Ministry of Education, School of Chemical Engineering and Technology, Tianjin University, Tianjin 300072, PR China

## HIGHLIGHTS

- ▶ Development of Ceria–salt composites with impressive ionic conductivity and tunable conduction behaviors is reviewed.
- ▶ Particular attention is given to ceria–carbonate composite, a promising electrolyte for LTCFC.
- ▶ Parameters affecting the electrical properties of ceria–carbonate composite are analyzed.
- ▶ Advanced applications, electrode materials and stability measurements development are presented.
- ▶ Novel fuel cell concepts and demonstrations such as EFFC are highlighted.

## GRAPHICAL ABSTRACT



## ARTICLE INFO

### Article history:

Received 5 August 2012

Received in revised form

14 December 2012

Accepted 21 January 2013

Available online 21 February 2013

### Keywords:

Low temperature ceramic fuel cells

Electrolyte-free fuel cells

Ceria–carbonate

Nanocomposite

Multi-ionic conduction

Transition metal oxide

## ABSTRACT

In the last ten years, the research of solid oxide fuel cells (SOFCs) or ceramic fuel cells (CFC) had focused on reducing the working temperature through the development of novel materials, especially the high ionic conductive electrolyte materials. Many progresses on single-phase electrolyte materials with the enhanced ionic conductivity have been made, but they are still far from the criteria of commercialization. The studies of ceria oxide based composite electrolytes give an alternative solution to these problems because of their impressive ionic conductivities and tunable ionic conduction behaviors. Significant advances in the understanding the ceria based composite material and construction of efficient fuel cell systems have been achieved within a short period. This report reviews recent developments of ceria-based composite from different aspects: materials, fundamentals, technologies, fabrication/construction parameters, electrochemistry and theoretical studies. Particular attention is given to ceria–carbonate (nano)composite, including its fuel cell performance, multi-ionic transport properties, advanced applications, corresponding electrode material and stability concerning. Besides, several novel fuel cell (FC) concepts like nanowire FC, all-nanocomposite FC and single-component/electrolyte-free fuel cell (SC-EFFC) are presented. This mini-review emphasizes the promise of ceria-based composites for advanced FC application and highlights the breakthrough of SC-EFFC research for high efficient energy conversion.

© 2013 Elsevier B.V. All rights reserved.

\* Corresponding author. Department of Energy Technology, Royal Institute of Technology (KTH), S-10044 Stockholm, Sweden. Tel.: +46 8 7907403; fax: +46 8204161.

\*\* Corresponding author. Tel./fax: +86 2227890481.

E-mail addresses: [liangd\\_fan@hotmail.com](mailto:liangd_fan@hotmail.com) (L. Fan), [cwywang@tju.edu.cn](mailto:cwywang@tju.edu.cn) (C. Wang), [binzhu@kth.se](mailto:binzhu@kth.se) (B. Zhu).

## 1. Introduction

Due to the ever increase energy demand and environmental deterioration, advanced energy conversion technologies have attracted growing attention during the last decades. Fuel cells are such kinds of electrochemical devices that convert chemical energy from fuel to electricity with specific characteristics of high efficiency and environmentally benign. There have been many kinds of fuel cell types since the invention of the first fuel cell by Grove [1]. For example, the proton exchange membrane fuel cell (PEMFC), alkaline fuel cell (AFC), phosphoric acid fuel cell (PAFC), molten carbonate fuel cell (MCFC) and solid oxide fuel cell (SOFC) [2].

SOFC or ceramic fuel cell (CFC), one of high-temperature fuel cells, has drawn the particular attention with PEMFC in the recent years because they show the most potential for nearly practicable application with the distinctive merits of high efficiency and low environmental impact. While SOFC shows some unique advantages compared with the PEMFCs, such as the multi-fuel choice and the fast electrode reaction rates originated from the high temperature operation. Thus, it has been considered as the fourth green energy conversion technology.

### 1.1. SOFC working principle

A typical SOFC contains three key components: anode, cathode and electrolyte. The all-oxide form effectively avoids some drawbacks, that is corrosion and needing of rigorous sealant compared with fuel cell with liquid components. In the SOFC, the electrolyte layer necessitates being dense and electronically isolating while providing a pathway for ion transport. It is sandwiched by two porous electrodes: anode and cathode, where the fuel oxidation reaction and the oxygen reduction reaction happen, respectively. Depending on the used electrolyte materials, SOFC is divided into oxygen ionic conductive SOFC (O-SOFC) and proton conductive SOFC (H-SOFC). The working principles of these SOFCs are shown in Fig. 1. Taking the SOFCs with an oxygen ion conductor as an example (Fig. 1b), hydrogen molecules dissociate and release two electrons at the anode. The electrons then move to the surface of the anode and transport to the cathode along the external circuit. While the oxygen molecule from the air is dissociated and ionized to oxygen ion when they combine with the electron from the anode. The oxygen ion will then transfer to the cathode/electrolyte interface and incorporate into the electrolyte and subsequently migrate within the electrolyte to the anode/electrolyte interface, and continuously moves to the reaction site. At the TPB, it meets with the proton to produce the water in form of steam. The water flows to the surface of anode and diffuses into the bulk gas of the exhausted fuel. The electron transport in the external circuit generates electricity and supplies the electrical power. At the same time, heat is produced due to the migration resistance of ion and electron as well as the reaction polarization loss. So the SOFC is a combined heat and power (CHP) generation. In addition, it should be pointed out that some composites and perovskite oxides electrolyte materials exhibit mixed oxide ion and proton conductivity in the fuel cell condition, so water is produced both at anode and cathode chambers in fuel cell condition.

### 1.2. Electrolyte materials in SOFC

In order to reach a good performance and improve the electrical efficiency of the fuel cell system, high ionic conductivity of electrolyte materials and super active electrode materials are desirable. Fortunately, with the fast evolution of functional materials and fabrication techniques in the last decade, satisfactory performances

have been achieved at intermediate to high temperature (600–1000 °C) range [3]. However, there is a worldwide trend to decrease the working temperature of SOFCs, current target of 500 °C even lower. The reduced temperature would let it more visible commercialization since it can effectively lessen the investment and operational cost as well as improve the system reliability [4–10]. Some other advantages such as the quickly start-up and shutdown and extend application fields, like portable devices, further stimulate the low temperature research activities [11–13]. As the heart of the SOFCs, the electrolyte plays a significantly important role in single cell performance. Two major solutions are developed in the recent years. One is to reduce the thickness of the electrolyte since the electrolyte ohmic loss is linearly proportional to this parameter [8,9,14]. Reducing the thickness of electrolyte allows the SOFC operation at a lower temperature with a fixed performance. The other is developing new high ionic conductive and stable electrolyte materials allowing to use a thick electrolyte layer which will benefit the cell fabrication process. Alternative electrolyte materials with improved properties have been uncovered. For instance,  $\text{Bi}_2\text{O}_3$  based materials [15],  $\text{Sc}_2\text{O}_3$  doped Zirconia [16],  $\text{Ca}_{12}\text{Al}_{14}\text{O}_{33}$  [17], doped  $\text{LaGaO}_3$  perovskite type oxide [18],  $\text{Ln}_{10}(\text{SiO}_4)_6\text{O}_3$  ( $\text{Ln} = \text{La, Nd, Sm, Gd and Dy}$ ) [19],  $\text{La}_2\text{Mo}_2\text{O}_9$  based fast oxide ion conductor [20], proton conductor like  $\text{BaZr}_{0.1}\text{Ce}_{0.7}\text{Y}_{0.2}\text{O}_{3-\delta}$  [21] and its derivatives  $\text{BaZr}_{0.1}\text{Ce}_{0.7}\text{Y}_{0.2-x}\text{Yb}_x\text{O}_{3-\delta}$  [22]. The conductivity plots of several ion conductive materials are shown in Fig. 2 [23,24]. However, these new developed materials show one or more specific drawbacks when they are used in the fuel cell condition. For instance, the phase structure change of bismuth oxide leads to the failure of cell [15]; the high reactive activity and extremely refractory of the doped  $\text{LaGaO}_3$  oxide make it hard to prepared thin film based fuel cells [25–27]. The state arts of electrolyte materials are still the cubic fluorite oxides, such as doped zirconia and ceria solid solution oxides. However, these cubic fluorite oxides shows either inadequate ionic conductivity below 700 °C or partial mixed conduction in the reduced atmosphere or at the elevated temperature [28,29]. Besides, as recommended by Etzell and Flengas [30], a critical value of ionic conductivity of  $0.1 \text{ S cm}^{-1}$  is needed to get a satisfactory fuel cell performance. Yet none of these materials' conductivities reach this value around 600 °C. Because of the structural factor, the ionic conductivities of these single-phase oxides cannot reach this value through the homogeneous doping. Therefore, developing new materials with the advanced ionic and stable properties is still in the research agenda.

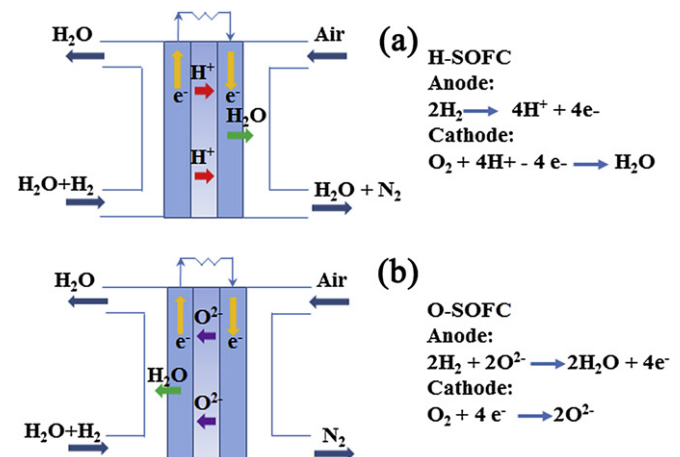


Fig. 1. Schematic of working principles for (a) proton and (b) oxygen ion conductive SOFCs, respectively.

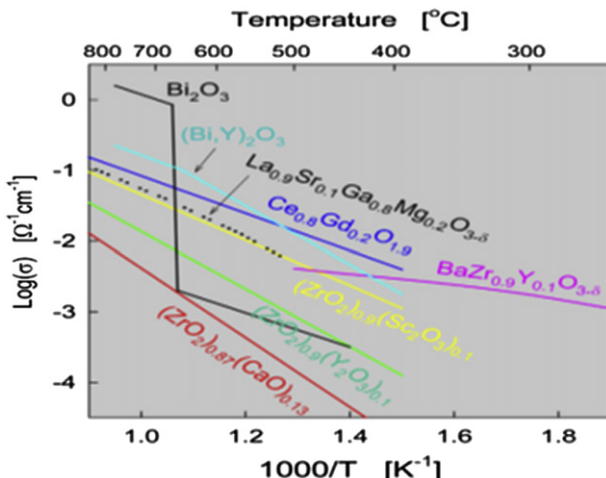


Fig. 2. Temperature dependence of electrical conductivity for oxide conductors [23,24]. Reproduced with permission from Copyright 2009, Elsevier.

### 1.3. Composite electrolyte

Recent work by Hui and the co-workers [31] have done a detailed review of the approaches for the ionic conductivity improvement on the selected electrolyte from the points view of material composition, microstructure and processing. They concluded that there was still absence of well qualified (phase stability and high ionic conductivity) single-phase electrolyte material at low temperature. Therefore, they suggested to vary the grain boundary conditions to improve the ionic conductivity of the single-phase electrolytes by introduction a liquid phase in the grain boundaries/interfaces forming the composite electrolyte. As an evidence, Fu and Zhu [32] had experimentally reported that GDC–LiCl–SrCl<sub>2</sub> showed a super-ionic conductivity improvement by 2–10 times compared with the doped ceria oxide alone between 400 and 600 °C. Schober [33,34] also demonstrated that the composites of oxide–carbonate/oxide showed the phase transition point that leaded to the marked ionic conductivity improvement, especially the proton conduction. Indeed, the composite approach has been used in many fields since the initiative work by Liang and his colleagues [35]. In their work, the ionic conductivity of lithium iodide is significantly raised by incorporating the second phase–aluminum oxide. The composite or heterogeneous doping concept has also been used in the high temperature and low temperature CFCs (HT/LTCFC) on the classical electrolyte materials. However, some technique barriers still exist before they are put into practical use [36–39]. Trade off phenomenon is observed in these composite electrolytes. For instance, the electronic conductivity of YSZ/GDC composite has been reduced with the increase of YSZ content, getting a satisfactory OCV value, while the fuel cell performance reduces due to the decreased total ionic conductivity [37].

A recent work by Garcia-Barriocanal [40] showed that remarkably electrical conductivity enhancement was observed at the interface of hetero-structural epitaxial ZrO<sub>2</sub>:Y<sub>2</sub>O<sub>3</sub>/SrTiO<sub>3</sub> thin film. However, the notably increased conductivity was determined to be the electronic nature by a combined characterization of the conductivity dependence on oxygen partial pressure and direct oxygen diffusion measurements [41]. Contrary to the two cases above, a serious work by Dr. Bin Zhu in the Royal Institute of Technology (KTH) of Sweden revealed a serious of two-phase composite electrolyte materials; and they are successfully employed as the advanced electrolytes for intermediate and low temperature SOFC

or CFCs application with high ionic conductivities and excellent fuel cell performances [42–47]. Ionic conductivity higher than 0.1 S cm<sup>-1</sup> was achieved above 300 °C and electrochemical power output higher 800 mW cm<sup>-2</sup> were earned at 600 °C with hydrogen as fuel [48,49]. Interesting, the composite electrolytes exhibit tunable electrically conductive properties, either proton or oxygen ionic or carbonate ionic conduction or mixed of them, depending on the specific gas conditions [44,50–61]. With the tunable electrical properties, the ceria–salts composites have been used for various applications beside the fuel cell function, such as the electrolysis mode, direct carbon fuel cell (DCFC), CO<sub>2</sub> separation and ammonia synthesis, as well as the electrochemical de-sulfur processes. All make the doped ceria based composites as the star-materials in energy and environmental fields.

### 1.4. Nanotechnology in composite electrolyte

The composite electrolytes generally contain two phases. One is the doped ceria oxide solid solution. The other is the salt or oxide phase, usually an insulating phase. It displays either a molten status such as the mixture of Li<sub>2</sub>CO<sub>3</sub> and Na<sub>2</sub>CO<sub>3</sub> above 500 °C or solid phase like Na<sub>2</sub>CO<sub>3</sub> and some oxides below the molten point. It has been demonstrated that the interface provides a highway channel for ionic transport, leading to an impressive ionic conductivity. In case of interface, two parameters should be considered. One is the interface density or the contact area between the two constitutions. The larger of the interface is, the higher electrical conductivity is. So reducing particle size of both phases will contribute to a higher ionic conductivity. More importantly, in nanostructured systems, the larger area of interface and/or grain boundaries will produce a high-density of mobile defects in the space-charge region [62]. On the other hand, the interaction between doped ceria and the second phase has also been of importance. Without the interaction between the two phases, the effective conductivity may reduce with the increase of the second phase. It also should be pointed out at here that the interaction here does not mean the chemical reaction rather with a physical nature since no new phase or ion diffusion between the two components happens. Fortunately, the high-energy surface of nanoparticles with large area of the interface is suitable for the interaction between two different compounds. Therefore, reducing the size of particle in the composite electrolyte will dedicate the final conductivity. The recent works on preparation and characterization of nanocomposite electrolyte have proved the higher ionic conductivity and lower superionic phase transition temperature point compared with the micro-level composite. Therefore, it is suggested that the nanotechnology will play an important role in the ionic conductivity improvement for future ionic conductive electrolyte material research.

Besides, nanostructured materials have been extensively explored as the functional components for advanced energy conversion and storage devices [62], such as the lithium-ion batteries, supercapacitors, solar cells and low temperature fuel cells [54]. The nanostructural materials have a significant fraction of grain boundaries and a large surface to volume ratio resulting in unique properties or combinations of properties as the functional components in a range of advanced energy devices. There is also great interest to use the nanostructure powder or materials in the high temperature fuel cells [14,62–66], especially the nanostructured solid conductors, known as “nanoionics” [67]. However, as said by Arico et al. [62] that one may start with nanosized particles in fabricating SOFCs materials, these are often modified by the high temperatures required for cell fabrication (>1000 °C), thus forming the microstructured components. In other words, the instability of the nanostructured materials becomes the major challenge to the SOFC community due to high temperature forming process. Though

the low temperature trend allows to use the nanosize materials more and more, the wide use is still at the beginning stage. In the ceria-based composite electrolyte, the ceria oxides are usual nanosize particles, while the grain growth of these nanoparticulates has been suppressed by the second phase. For instance, the ceria oxide core in the core–shelled ceria–carbonate composite has been surrounded by the carbonate shell, which could undergo a severe high temperature heat treatment without particle size increase [48,68]. There is also another concerning, i.e. the nanosize effect. As suggested by Maier, the “trivial” size effect and the “true” size effect make up of the total size effect. The trivial size effect results from the sum of the interface, as mentioned above. Dissimilarly, the true size effect occurs when the particle size is close to the Debye length. At the interface, the local electrical property changes completely, even from ionic to electronic conduction behaviors [69]. The mixed ionic and electronic conductive behavior of doped ceria oxides has been widely discussed under the reduced particle size and dimensions [70–72]. In the ceria–salt composite electrolyte systems, the electronic conduction of the nanocrystalline ceria has been ruled out so that the composites keep a unit ion conduction transport number at the applied atmospheres and temperature [58,73].

Thus, this mini-review describes some recent advances in developing ceria-based nanocomposite electrolyte for reduced temperature CFCs in term of materials synthesis, physical characterization to the electrical conductivity and fuel cell performance. Priority has been given to the ceria–carbonate composites. The multi-ionic conduction behaviors are discussed with other advanced applications. Some advanced concepts and device demonstrations originated from the nanocomposite research are also presented. The electrode materials development and stability performance results related with the ceria based composite are reviewed. Although there have already several review papers published in this field [43–47,74,75], most of them are from the material design aspect or the latest three year literature survey. Hence, there is an urgent need for one comprehensive survey on developing ceria based composite ionic conductors for low temperature SOFCs/CFCs. At the same time, the fundamental issues of the recent breakthrough research-single-component/electrolyte free fuel cells (SC/EFFCs) are also mentioned in this work. This study here will help to understand and prospect the potential of ceria-based composite materials for advanced energy conversion and environmental applications.

## 2. Ceria-based (nano)composite electrolyte

Generally, the ionic conduction in single-phase materials follows the oxygen vacancy mechanism. However, the limited oxygen

vacancies (limited charge carriers) and the long transport distance (high activation energy) restrict the final ionic conductivity. Although the oxygen vacancy concentration can be enhanced with the increase of the doping content, there is an optimal value, above that the oxygen sublattice ordering caused by the defect association or interaction may reduce and subsequently do a detrimental effect on the electrical conductivity.

In recent years, a series of functional two-phase ceria–salts (nano) composite materials have been exploited to overcome the low ionic conductivity of single-phase electrolyte materials [43–46,74]. For example, ceria–carbonate [43,48,56–58,76–79], ceria–halide [32,42,80,81], ceria–sulfate [82], ceria–hydroxide [42,83] and ceria–oxide [51,84–87] are widely explored and tried as the electrolytes for low temperature CFCs. The ceria oxides in composite electrolytes are either SDC or GDC or YDC. The ionic conductivities of these composite electrolytes are much higher than those of the single-phase doped ceria or zirconia oxides, as shown in Fig. 3a. Taking the doped ceria– $\text{Na}_2\text{CO}_3$  as an example, its ionic conductivity can reach  $0.1 \text{ S cm}^{-1}$  around  $300^\circ\text{C}$ , which is two orders of magnitude higher than that of single-phase SDC material (Fig. 3b). Besides, unlike the linearity of the Arrhenius plots for the single-phase electrolyte materials, the conductivity of the ceria–salt composite electrolyte shows an obvious discontinuity at one temperature-point or range, which is defined to the superionic phase transition [33,34]. Most ceria based composite electrolyte follows this trend, even for the all-oxide nanocomposites. The superionic ionic phase transition highly depends on the composition and the operational condition, such as the temperature raising rate and the applied gas atmosphere. While the  $\text{Y}_2\text{O}_3$ –SDC nanocomposite developed by Rizwan [85] does not show any conductivity jump at all the temperature range but still displays much enhanced conductivity in comparison with SDC.

In the following paragraphs, two kinds of nanocomposites will be described in details. One is the ceria–carbonate nanocomposite electrolyte, the other is the ceria–oxides nanocomposite. The ceria–carbonate stands for the mainstream of research because of its amazing properties and achievable excellent electrochemical performance, while the ceria–oxide composite research represents the further development direction for advanced applications.

### 2.1. Ceria–carbonate (nanocomposite)

Among these composite electrolytes, doped ceria–carbonate shows the most promising potential compared with other doped ceria–salt composites [43,48,56–58,88,95]. As a matter of fact, the research on the doped ceria–carbonate has excited worldwide interesting with great progress in the recent years both on the ceria–carbonate composite themselves [52,54,55,59,60,75,83,88,90–

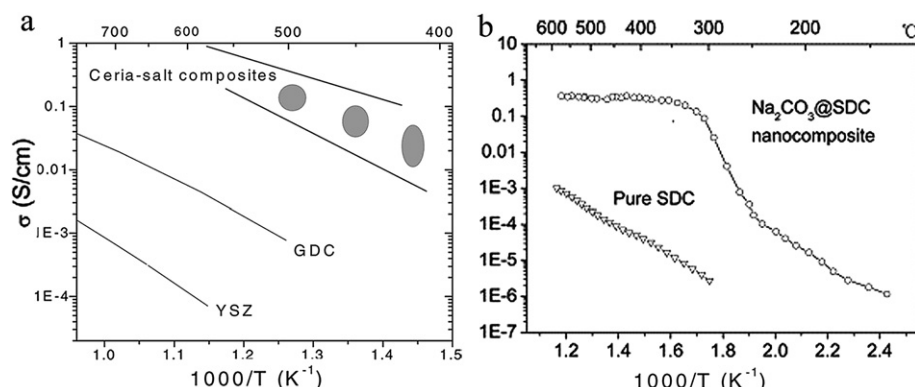


Fig. 3. Electrical conductivity of (a) ceria-salts composite and (b) ceria-carbonate composite. (Taken from Refs. [43,48] with permission of Elsevier).

93,96–117] and on the high performance fuel cell and electrode development [92,118–137]. The typical microstructures of ceria–carbonate composite are shown in Fig. 4. The TEM image (Fig. 4a) shows a clear core–shell structure with the ceria oxide as the core and carbonate as the shell component. More interesting, the carbonate shows obviously an amorphous structure compared with the clear crystalline of ceria oxide at room temperature. In addition, one may see that the interface phase is clearly different from both the amorphous carbonate and crystal SDC. And this interface is suggested to build the high-speed way for ionic conduction and interfacial function in these composite electrolytes. The high-resolution SEM images shown in Fig. 4b doped ceria nanoparticles are homogeneously surrounded by the carbonate. In addition, the doped ceria shows narrow particle size distribution, which can be easily synthesized by a wet-chemistry method, such as the co-precipitation and combustion processes. In addition, the early stage composite has displayed a good sintering density. The interface conduction mechanism will be discussed in the next section of this paper. The electrolyte functions of ceria–carbonate nanocomposites have been demonstrated by many groups for low temperature CFCs with excellent fuel cell performances as listed in Table 1. For example, fuel cells using Ni-based electrodes and SDC–(Li/Na)<sub>2</sub>CO<sub>3</sub> composite electrolyte reached a power density of 1085 mW cm<sup>−2</sup> and OCV higher than 1.0 V using hydrogen as the fuel and air as the oxidant [52]. Higher performance of 1200 mW cm<sup>−2</sup> is also achieved when the air is replaced with the O<sub>2</sub>/CO<sub>2</sub> mixed gas at 600 °C [55]. More importantly, a recent work by Rizwan reported that a peak power density of 1150 mW cm<sup>−2</sup> can be obtained with the nanocomposite homogeneous SDC–Na<sub>2</sub>CO<sub>3</sub> prepared by a simple one-step co-precipitation method at 500 °C [49]. The improved performance and the reduced material and system preparation process make the ceria–carbonate nanocomposite more valuable for practical applications [138]. The electrochemical performances are much higher than that of SOFC with much thinner SDC and MCFC with  $\alpha$ -LiAlO<sub>2</sub>–(Li–K)<sub>2</sub>CO<sub>3</sub> electrolyte. The results demonstrate the great potential of ceria–carbonate composite as the functional electrolyte for low temperature CFCs.

### 2.1.1. Effects of the fabrication technologies

Two typical ways are employed to prepare the ceria–carbonate (nano) composites as shown in Fig. 5. The mechanical mixing is the most common used method while the infiltration method is newly developed with the initial intent to improve the mechanical strength of this composite [103,110,139]. In case of mechanical mixing, ceria oxide and carbonate are separately prepared and then mixed with each other followed by high temperature (above the molten temperature of carbonate composite) annealing. While for the infiltration way, a porous SDC substrate is prefabricated followed by the immersing the porous SDC matrix into the molten

carbonate composite. Ceria–carbonate composites by various fabrication methods show clearly different microstructures (Fig. 5a and b). The ceria oxide and carbonate are homogeneously distributed and the ceria oxide is generally surrounded by carbonate since the molten carbonate can easily move and cover the surface of the ceria oxide during the calcination. However, a clearly separated doped ceria and carbonate structure can be identified as displayed in Fig. 5b for the samples by the infiltration process [103]. The carbonate resides in the left pores of the porous SDC skeleton. The continuous oxide and carbonate phases as well as the interfaces induced by the interconnected porous structure will provide larger channels and highways for ion transport in the ceria–carbonate composite. Therefore, a higher AC conductivity of 0.46 S cm<sup>−1</sup> at 600 °C was reported based on this novel structure compared with the mechanical mixing [103]. In addition, the composite electrolytes by molten salt infiltration show much lower activation energies both at high and low temperature ranges than those of mechanically mixed composites [110]. The composite electrolyte by the infiltration approach with superior performance shows promising application in future SOFC R&D and other applications, like CO<sub>2</sub> separation. Nevertheless, the performance of such a novel microstructural composite electrolyte has not yet tested for low temperature CFCs.

Due to the complex multi-step fabrication process (co-precipitation–calcination–mixing–calcination–crushing) of the mechanical mixing method, Wang et al. [48] first reported a wet-chemical way to prepared the ceria–carbonate core–shell structural nanocomposite. The co-precipitated ceria precursor is directly mixed with Na<sub>2</sub>CO<sub>3</sub> in a water solution, and then they are subjected to drying and calcination steps to form the final nanocomposite. Recently, they also [49] developed a more facile one-step co-precipitation technique to produce the nanocomposite electrolyte. The precursor of the new formed metal-ionic hydroxide or metal-ionic carbonate by co-precipitation process could absorb the excess Na<sub>2</sub>CO<sub>3</sub> and undergo a heat-treatment process to form the final ceria oxide–Na<sub>2</sub>CO<sub>3</sub> nanocomposite. This kind of ceria–carbonate nanocomposite shows excellent ionic conductivity and fuel cell performance as the electrolyte for low temperature CFCs. However, the one-step co-precipitation method is difficult to control the content of residual carbonate in the composite, while the thickness of carbonate shell is vital for the electrical properties. Whereas, the simple preparation process, homogeneous structure plus the superior ionic conductivity may contribute the industrial scale-up of this advanced nano composite electrolyte.

Ceria–carbonate composite was also prepared with a structure of alternate GDC and (Li/Na)<sub>2</sub>CO<sub>3</sub> layer (up to seven layers) by Saradha [116] to identify the role of interface between the two components. The pellet impedance responses both at series and at parallel associations in air were studied and compared with the

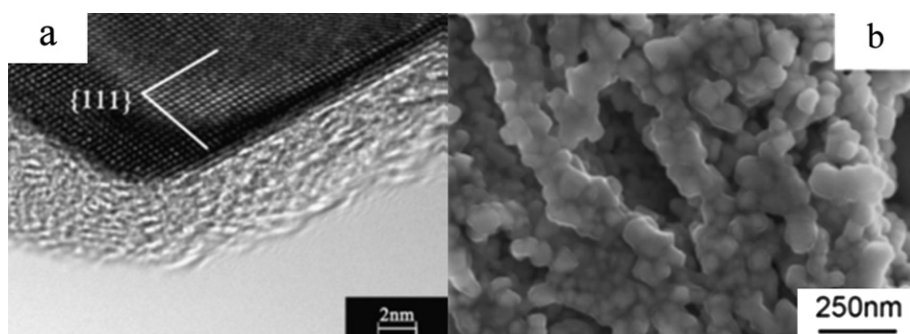


Fig. 4. (a) TEM images and (b) SEM images of ceria–carbonate nanocomposite (Taken from Refs. [48,95] with permission of Elsevier).

**Table 1**

Electrochemical performances of CFCs with ceria–carbonate nanocomposite electrolyte from different research groups. Ni and lithiated NiO are used as anode and cathode catalysts, respectively, unless otherwise stated. The electrochemical performances of SOFC with thin film doped ceria and molten carbonate fuel cells (MCFCs) with  $\text{Al}_2\text{O}_3$ –( $\text{Na}_2\text{CO}_3$ ) are included for comparison.

Group	Electrolyte composition <sup>c</sup>	Performance ( $\text{mW cm}^{-2}$ )		Note	Refs.
		450 °C	600 °C		
B. Zhu in KTH	SDC–20(Li/Na) $_2\text{CO}_3$	50	590	One-step co-precipitation SDC nanowire	[56]
	SDC–20 $\text{Na}_2\text{CO}_3$	600	—		[48]
	SDC– $\text{Na}_2\text{CO}_3$	1000	—		[49]
	SDC–20 $\text{Na}_2\text{CO}_3$	160	522		[78]
ZQ. Mao from Tsinghua Univ.	SDC–20(Li/K) $_2\text{CO}_3$	330	560	[88] [52] [89]	[88]
	SDC–25(Li/Na) $_2\text{CO}_3$	400	1085		[52]
	SDC–20(Li/Na) $_2\text{CO}_3$	—	600		[89]
	SDC–(Li/K) $_2\text{CO}_3$	525	—		
	SDC–20(Na/K) $_2\text{CO}_3$	550	—		
M. Cassir from Chimie ParisTech	GDC–20(Li/K) $_2\text{CO}_3$	—	60	—	[90]
S. Basu from Indian	GDC–25(Li/Na) $\text{CO}_3$	45	—	—	[91]
YD. Li at Tianjin Univ.	SDC–30(Li/Na/K) $_2\text{CO}_3$	—	420	CO <sub>2</sub> /O <sub>2</sub> cathode gas	[54]
SW. Tao from UK	SDC–30(Li/Na) $_2\text{CO}_3$	—	1200	—	[55]
SA Song et al.	$\text{Ce}_{0.8}\text{Gd}_{0.05}\text{Y}_{0.15}\text{O}_{1.9-40}(\text{Li/Na})\text{CO}_3$	—	204/370 <sup>a</sup>	$\text{Sm}_{0.5}\text{Sr}_{0.5}\text{Fe}_{0.8}\text{Cu}_{0.2}\text{O}_{3-\delta}$ cathode	[92]
	$\text{Ce}_{0.8}\text{Gd}_{0.05}\text{Y}_{0.15}\text{O}_{1.9}$	43	670 <sup>b</sup>	—	[93]
SA Song et al.	$\alpha\text{-LiAlO}_2$ –(Li/K) $_2\text{CO}_3$	—	155 <sup>b</sup>	—	[94]
	—	—	159	—	[94]

<sup>a</sup> Performance of single cell before and after short-term testing.

<sup>b</sup> 550 °C, composite electrolyte thickness 1.2 mm,  $\text{Ce}_{0.8}\text{Gd}_{0.05}\text{Y}_{0.15}\text{O}_{1.9}$  thickness 70  $\mu\text{m}$ , the identical testing condition.

<sup>c</sup> The number before carbonate means weight ratio of carbonate in the composite.

single component and the mixed phase, but they concluded “no sign of special contributions originated in the ceramic/salt interface”. There may be two reasons. One is the limits of the AC impedance. All the ions can contribute to the final micro-level impedance response, making it hard to separate the contribution from the oxygen ion conduction [58,61]. The other is the micro-structure of the alternate structure of composite. Since a low sintering temperature is used, the SDC layer may give large porosity.

The molten carbonate will penetrate the porous SDC leading to a similar structure with materials by mechanical mixing method and a similar electrical response under AC condition. Carefully microstructure manufacture is therefore needed to make such claims. Besides, in their work, the electrode impedances shown distinct and unique characteristics between different cells, still suggesting the possibility of the interface role in the ionic conduction [116].

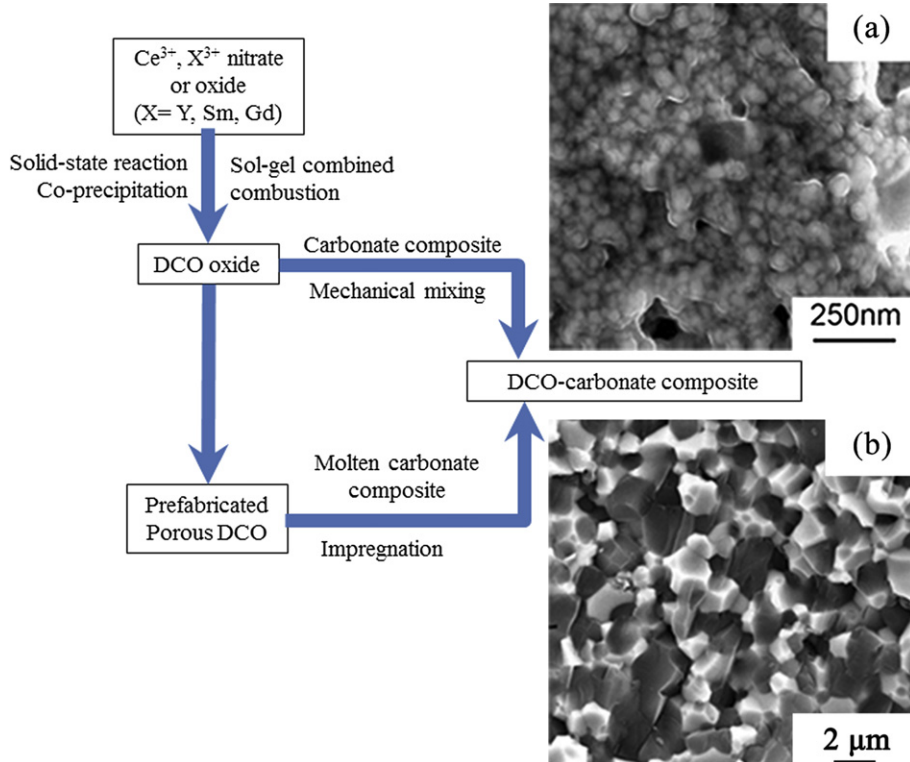


**Fig. 5.** Two typical ceria–carbonate composite fabrication processes and the resulted different microstructure: (a) by mechanical mixing and (b) by infiltration. Taken from Refs. [95,103] with permission of Elsevier.

### 2.1.2. Effects of carbonate composition and content

Table 1 lists the electrochemical performances of low temperature ceria–carbonate composite based CFCs from different groups. It clearly shows the discrepancies from different carbonate compositions and contents. It should be noted that the performances of composites are highly depended on the microstructure as well as other parameters, such as the particle sizes, morphologies, the applied gas environment etc., not only the composition. However, most peak power density of low temperature CFCs with ceria–carbonate composite electrolyte are much higher than that of SOFC with doped ceria oxide single-phase electrolyte or MCFC with  $\text{Al}_2\text{O}_3$ –carbonate composite electrolyte [93,94].

To find the effects of carbonate composition on the electrical properties of ceria–carbonate, the same preparation and measurement conditions should be ensured. Besides, the sample environment, e.g. testing environment or gas atmosphere, are vital due to extrinsic nature of the ceria composite materials [113]. Huang et al. [89] investigated the electrical performances of  $(\text{Li}/\text{Na})_2\text{CO}_3$ ,  $(\text{Li}/\text{K})_2\text{CO}_3$  and  $(\text{Na}/\text{K})_2\text{CO}_3$  and the results are shown in Fig. 6. The AC conductivities in air and electrochemical performance in  $\text{H}_2$ –air condition are compared. A sharp conductivity leap appeared at 475 °C and 450 °C for composite electrolyte with  $\text{Li}_2\text{CO}_3$  and another carbonate. However, the conductivities of SDC– $(\text{Na}/\text{K})_2\text{CO}_3$  increased linearly with temperature and one order of magnitude lower than that of SDC (composite precursor) at the entire testing temperature range. However, the power densities of single cells based on above composite electrolytes by dry-pressing technique did not follow the trend of the conductivity. Single cells with SDC– $(\text{Li}/\text{Na})_2\text{CO}_3$  show the highest power output between 500 °C and 600 °C. The performances of single cells with SDC– $(\text{Li}/\text{K})_2\text{CO}_3$  and SDC– $(\text{Na}/\text{K})_2\text{CO}_3$  electrolytes are close but are still much higher than those of SDC based fuel cells. It can be concluded that they are different for ionic conduction behaviors, charge carriers and their transport pathways for ceria–carbonate composites respectively in air or in fuel cell conditions.

The influence of carbonate content in the ceria–carbonate composite on the DC oxygen ionic conductivity was investigated by Liu et al. [108] since the AC conductivity contains the contribution of all mobile ions,  $\text{O}^{2-}$ ,  $\text{CO}_3^{2-}$  and cation ions ( $\text{Li}^+$  and

$\text{Na}^+$ ). They found that the DC conductivity is not directly proportional to the carbonate content (10–40 wt%). Instead, there is an optimum value 80:20 of SDC to carbonate, higher carbonate content leads to reduction of electrical conductivity both at low and high temperature ranges. In addition, the super-ionic phase/conduction transition point changed with the content of carbonate. Moreover, an oxygen ionic conductivity of  $0.01 \text{ S cm}^{-1}$  was obtained at 480 °C, which can be only realized at 600 °C for SDC and 800 °C for YSZ electrolyte, indicating the enhanced oxygen ionic conduction compared with the single-phase ionic conductors.

### 2.1.3. Effects of the sintering temperature

The electrical properties of the ceria–carbonate composite are also highly depended on the microstructure. The composites are normally working at the temperature range of 500–600 °C. At this temperature, the carbonate is a molten state (liquid phase). Its physical and chemical properties will change with the applied temperature. So the effect of temperature on the microstructure and the consequent electrical properties are studied by Xia and the co-workers [104]. They found that the samples sintered at 675 °C showed the best microstructure: homogeneous compound distribution and compact contact between ceria oxide and carbonate with less porosity. Lower temperature results in a high porosity while higher temperature leads to large disconnection between two constituents as shown in Fig. 7. The best microstructure of ceria–carbonate sintered at 675 °C also gives the highest conductivities, both grain conductivity and the grain boundary conductivity. In addition, the grain boundary (GB) conductivities of these composites are higher than bulk conductivities. Therefore, the GB conductivity makes the primary contribution to the total ionic conductivity, which is inherently different from the single-phase electrolytes such as the SDC, in which the grain boundary results in high resistance and limits the overall ionic conductivity.

### 2.1.4. Effects of SDC particle size and morphologies

As mentioned above, the interface plays an important role in the electrical performance of the ceria–carbonate. Reducing the SDC particle size will enhance the contact area of ceria and carbonate, giving a high-density interface that is expected for an improved electrical performance. In addition, the continuing network may provide a long-term order pathway for ionic transport, such as the ceria–carbonate composite prepared by the infiltration method. The SDC materials with long-term order structure such as the nanowire, nano-rod may also give more possibilities to the high electrochemical performance.

Gao et al. [140] tested the electrochemical performances of fuel cells with SDC– $\text{Na}_2\text{CO}_3$  composites (SDC particle sizes less than 100 nm and few micrometers, respectively) in fuel cell condition. The electrical conductivities of different composite electrolytes are calculated according to the  $I$ – $V$  characteristics. They showed that the conductivity of the SDC/ $\text{Na}_2\text{CO}_3$  nanocomposite is several times higher than that of the SDC– $\text{Na}_2\text{CO}_3$  micro-composite. Tang [141] and Fan [142] also prepared three kinds of SDC– $(\text{Li}/\text{Na})_2\text{CO}_3$  composites with different particle sizes from micrometer level to tens of nanometer levels. The electrical behaviors were investigated by the impedance analysis. The nanocomposite shows the more complex grain boundary interfacial effects than that of composite with micro-level grains; and the nanocomposite displays higher AC conductivity and lower activation energy, especially at low temperature range. Therefore, the doped ceria–carbonate composite with reduced ceria particle size shows superior performance.

In order to compare the electrical behaviors of ceria–carbonate with different SDC particle morphologies, SDC powders were prepared by glycine-nitrate combustion (GN), oxalate-co-precipitation

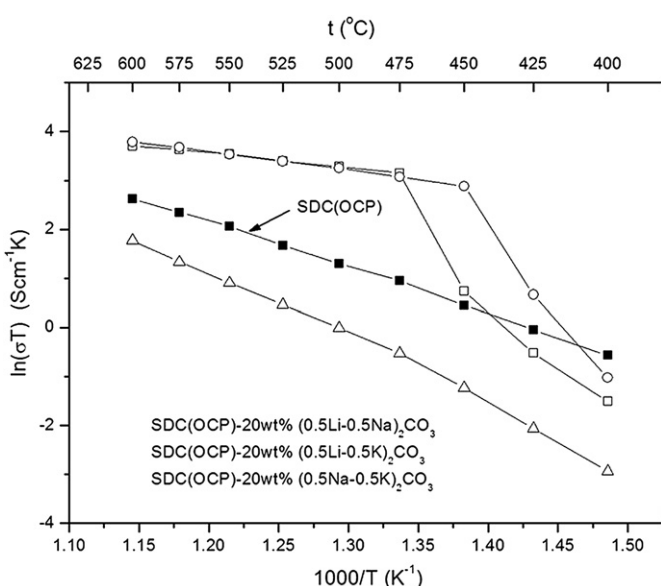


Fig. 6. Arrhenius plots of composite electrolytes with different carbonate compositions [89].

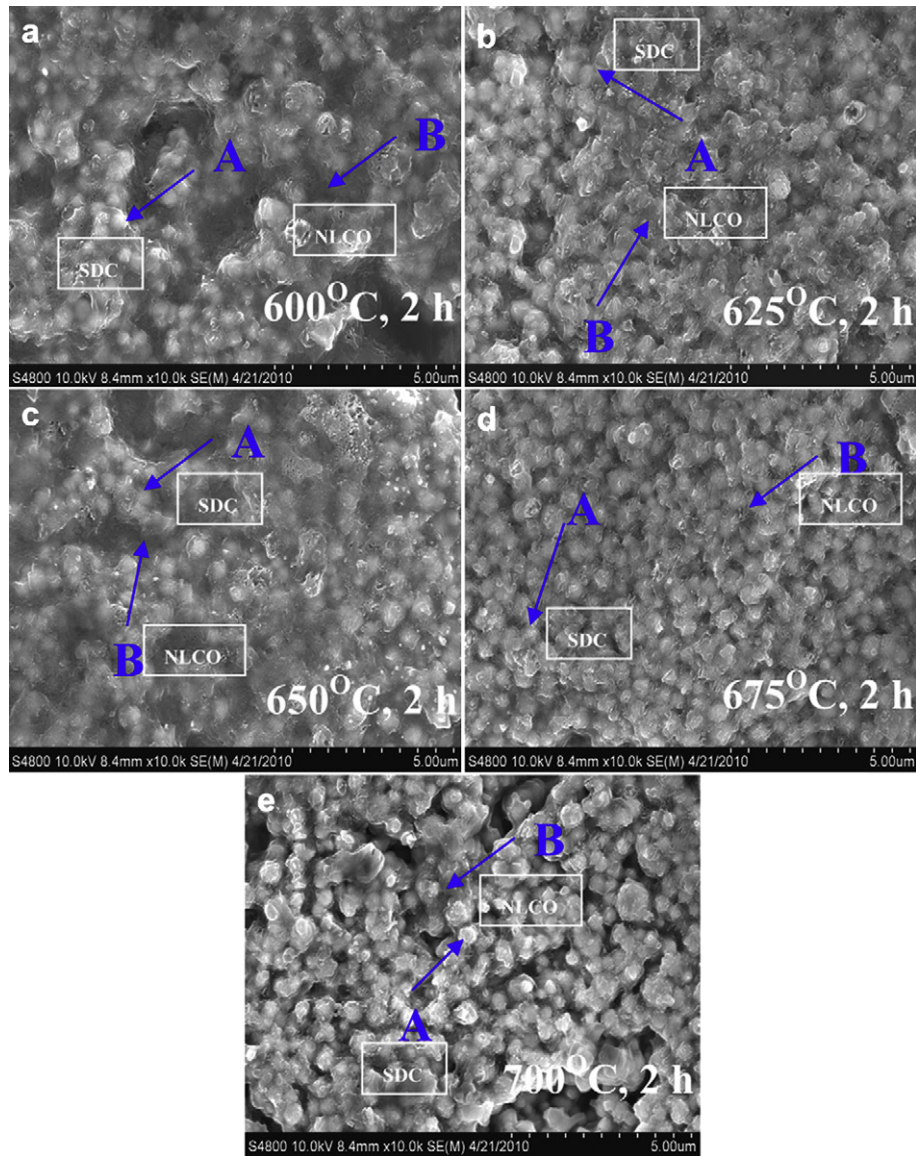
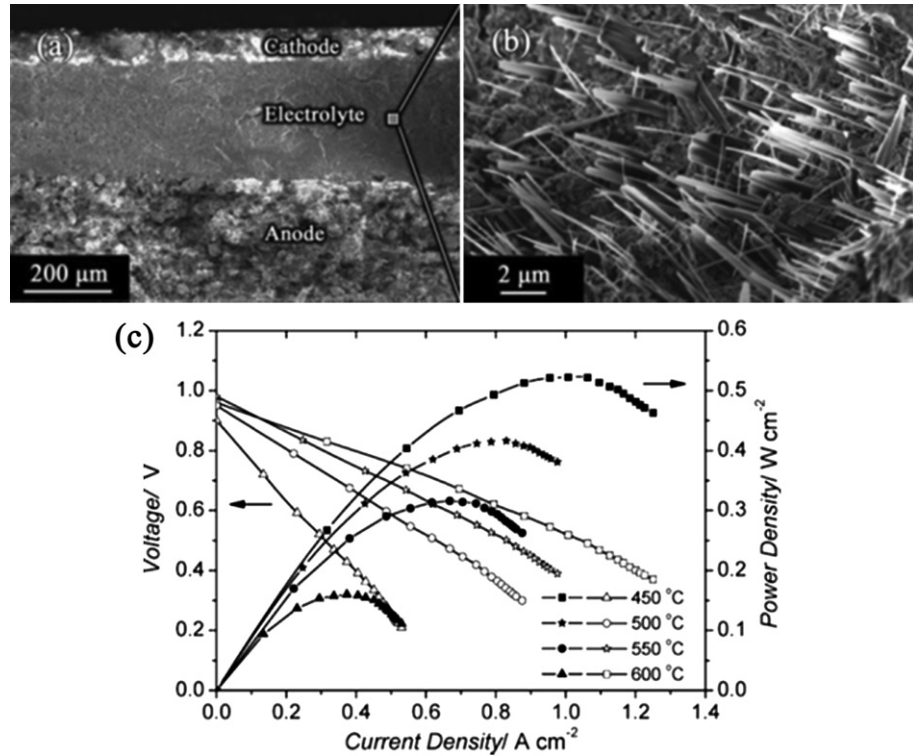


Fig. 7. Temperature dependence of the microstructures of the ceria–carbonate in air [104].

(OC) and sol–gel process (SG) by Xia and his co-workers [55], respectively. The GN process gives a porous foam-like structure, the OC samples show a rod-like shape, whereas the SG powder consists of aggregates. The SDC and composite originated from GN give the largest specific surface area and crystal size, while SG process shows reverse results. After mixing with carbonate, the OC sample shows the best conductivity while GN process gives the lowest one. However, all of them are higher than that of the SDC sample at the temperature range of 300–650 °C. The maximum power densities of 1266, 1121 and 607 mW cm<sup>−2</sup> were obtained for fuel cell with ceria–carbonate composite electrolyte from the OC, SG and GN processes, respectively. Based on these results, it seems that the SDC–carbonate with a rod structural SDC precursor gives the best conductivity and fuel cell performance because of the long-term order structure that facilitate the ion transport in the composite electrolyte. The larger surface may provide tortuous path and negative effect for ionic migration. Of course, the composite status, the carbonate volume and the porosity of the composite electrolyte should be considered before making an effective comparison of the electrical properties.

### 2.1.5. Novel ceria nanowire–carbonate nanocomposite

As been stated, the ceria–carbonate with long-order grain-boundaries/interfaces may facilitate the ion transport, leading to high ionic conductivity and thus the high fuel cell performance. Therefore, a recent interesting work by Ma et al. [78] reported that low temperature CFCs was made with the SDC nanowire–carbonate composite electrolyte. The SDC nanowire was synthesized by a novel chemical synthetic route with large quantities. The use of the second phase could help to stabilize the one dimension nanowire structure that can survive at such a rigorous environment: high temperature and redox gas atmosphere. The cross-section microstructures of the prepared cell are shown in Fig. 8a and b. It can be seen from Fig. 8b, the nanowire structure of SDC has been well preserved after the cell performance testing. A good fuel cell performance of 522 mW cm<sup>−2</sup> is achieved at 600 °C with an electrolyte thickness of 200 μm. One task for the nanowire based composite electrolyte is to arrange of the orientation/align of the nanowire, in order to get large and continuous interface and to maximize the effective ionic conductivity and fuel cell performance.



**Fig. 8.** (a, b) SEM images of single SOFC with doped ceria nanowire–carbonate electrolyte and (c) the corresponding electrochemical performance. Reprinted from Ref. [78] with permission. Copyright 2010 Wiley.

### 2.1.6. All nanocomposite ceramic fuel cells

One of the distinct advantages of the ceria–carbonate composite as the electrolyte for CFCs is the low sintering temperature, as low as 600 °C. The low temperature fabrication effectively reduces the detrimental reaction between different cell components and nanoparticle grain growth as well as electrode sintering. Thus, large triple phase boundaries where the electrochemical reactions take place from the compacted nanoparticles are maintained, inducing to a high electrode catalytic activity. As a result, the nanostructured electrodes can be used in this kind of fuel cells at low temperatures.

In one of the recent publications, low temperature CFC based on all-nanocomposite materials was proposed and demonstrated by L. Fan and his colleagues [79]. The nanostructure Ni–Fe/SDC, SDC–(Li/Na)<sub>2</sub>CO<sub>3</sub> nanocomposite and lithiated NiO/ZnO were used as the anode, electrolyte and cathode, respectively as shown in Fig. 9a–c, respectively. Fuel cells were prepared by a co-pressing technique, in situ sintering and tested in hydrogen/air condition. Power density of 550 mW cm<sup>-2</sup> was achieved at 600 °C. Besides, the performance and the electrode microstructure kept stable in the thermo-cycle testing.

### 2.2. Ceria–oxide nanocomposite

Some years ago, Zhu and Schober et al. [33,51] investigated SDC–BaCe<sub>0.8</sub>Y<sub>0.2</sub>O<sub>2.9</sub> all oxide composite electrolyte system. These all-oxide composite electrolytes also exhibited similar superionic conductivity with ceria–salts based composite. In last two years, some all-oxide nanocomposites were also developed to overcome the inherent instability properties of carbonate in the ceria–carbonate composite, such as the volatilization and the decomposition in the severe working environments. these samples are SDC–LiZnO [84] and SDC–Y<sub>2</sub>O<sub>3</sub> [85,86,143] which have a similar

structure, like the core–shell structure as shown in Fig. 10. The HRTEM image of SDC–LiZnO (Fig. 10a) showed that LiZn-oxide with the *d*-spacing of (401) plane of 0.267 nm surrounded around the doped ceria. The SDC–Y<sub>2</sub>O<sub>3</sub> nanocomposite also shows a thin layer of Y<sub>2</sub>O<sub>3</sub> on the surface of the doped ceria with a narrow particle size distribution (the inset of Fig. 10b). These all-oxide-nano-composites display much higher (1–2 orders of magnitude) electrical conductivities than pure SDC and promising electrochemical performance as the electrolyte for low temperature CFCs. For instance, a high fuel cell power density of 630 mW cm<sup>-2</sup> at 520 °C was obtained for CFC with SDC–LiZnO nanocomposite electrolyte [84]. Oxide nanocomposite electrolytes with significantly improved physicochemical stability and enhanced electrical property are expected to make a breakthrough in low temperature CFCs materials and technology. More oxide nanocomposites are needed for future high ionic conductive electrolyte development, where the nanocomposite concept may be followed to build large interfaces for super functionalities.

### 3. Multi-ions conduction and advanced applications

The excellent electrical properties have made doped ceria-based composites star materials in the low temperature CFC field. The ionic conduction mechanism has also become a hot topic in recent years and has been extensively investigated from different research groups [43,52–59,88,113,144]. Note that the composite approach not only improves the overall ionic conductivity but also largely introduces the proton conduction in fuel cell condition or in hydrogen and humidified atmospheres [52,53,56–58,145]. It has been proved that CFCs with proton conduction show a higher theoretical efficiency and lower activation energy compared with the oxygen ion transport in the solid-state ion conductor [146]. Some works also proved that the presence of CO<sub>2</sub> in the cathode

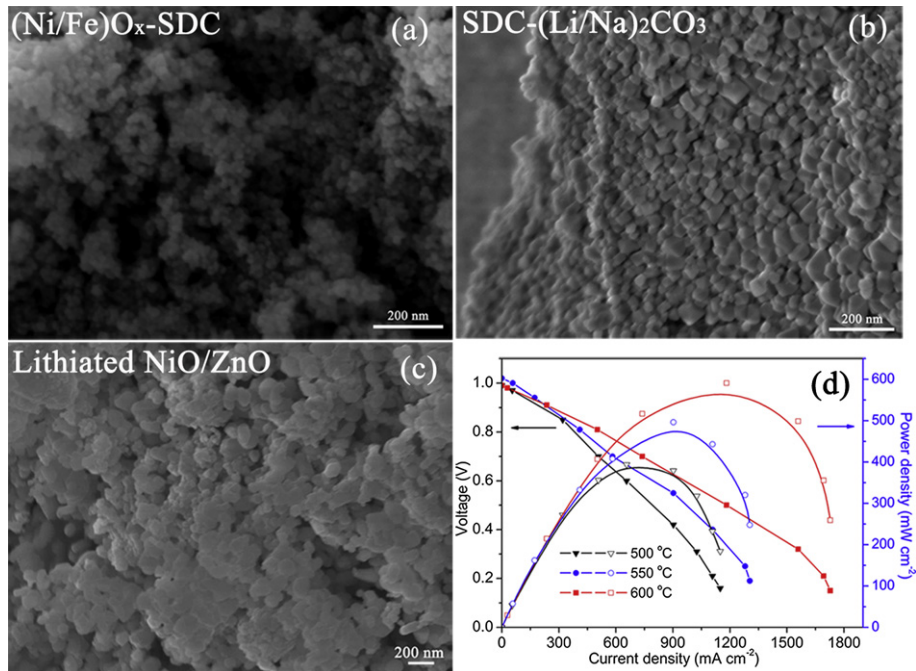


**Fig. 9.** A low temperature ceramic fuel cell constructed with all nanocomposite materials showed promising performance below 600 °C [79].

atmospheres promotes the total ionic conduction in the ceria–carbonate (nano) composite electrolyte [54,55,59]. The multi-ion conduction could significantly enhance not only the ionic conductivity but also extend the possible some other advanced applications in energy and environmental fields. In this section, various methods to validate the multi-ion conduction behaviors are first introduced; then the suggested ionic conduction mechanisms in the open literatures are summarized.

### 3.1. Versatile techniques to study the multi-ionic conduction behaviors

In the past several years, various methods have been used to identify the multi-ionic conduction properties in the ceria-based composite electrolyte. In fuel cell condition, the simple way to study the multi-ionic conduction behaviors is through the experimental observation: water produced both sides of the electrode chambers as reported by works [43,53,57,88]. One may argue that

the water produced in the cathode is the result of the hydrogen leakage through the porous electrolyte layer. But we should recognize that high OCV values close to the Nernst values are frequently observed. More important, Huang [53] found that the ceria–carbonate composite could be a pure proton conductor based on that all the water was observed in the outlet gas of cathode chamber. The simple experimental observation reveals the mixed proton and oxygen ionic conduction in ceria–carbonate composite under fuel cell condition. However, this method is difficult to quantitatively analyze the contribution of different charge carriers, the proton or the oxide ion.

Concentration cell measurement is another common way to analyze the ionic conduction behaviors of solid-state ion conductors and composite materials [19,147–150]. Zhu et al. [73] found that the SDC–(Li/K)2CO3 composite was a mixed  $\text{CO}_3^{2-}$ , oxygen ion and proton hybrid conductor using the carbon dioxide and vapor concentration cells. The carbonate ionic transport dominated the total ionic conductivity with transport number about 0.67 above

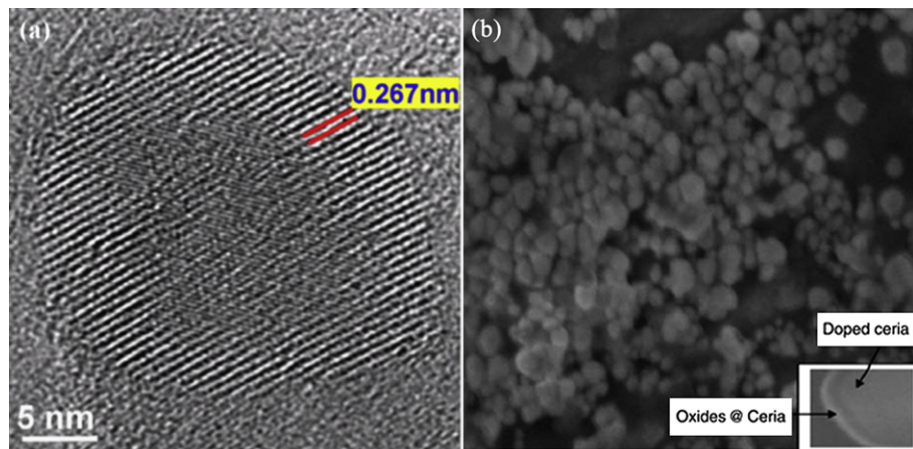


**Fig. 10.** Electron microscopy of (a) SDC–LiZnO [84] and (b) SDC–Y<sub>2</sub>O<sub>3</sub> [85,86] nanocomposite electrolyte. With permission from Elsevier.

500 °C and the oxide ion transport number of 0.31 at 500 °C. The proton conductivity is much lower compared with those of the carbonate and the oxygen ions. Di et al. [56] found that the OCVs of the ceria–carbonate composite electrolyte based fuel cell decrease with the increase in water content of either anodic or cathodic inlet gas, suggesting the hybrid proton and oxygen ionic conduction behaviors in the composite. And they found that the effect of oxygen ionic conduction was more significant than that of proton conduction. The concentration cell measurements also demonstrate that the ceria–carbonate composite is a mixed ionic conductor, its specific ionic conduction may be utilized for different application.

AC impedance analysis or electrochemical impedance spectrum (EIS) is generally used to study the ionic conduction behavior of solid-state ion conductor. However, it should be noticed that the electrochemical impedance response of the ceria–carbonate composite contains the contribution of all mobile ionic species, which make it complex to determine each specific ionic contribution [106]. However, the EIS is still useful for qualitative analysis. Fan et al. [57] found that the ohmic intercept on the real axis of SDC–(Li/Na)<sub>2</sub>CO<sub>3</sub> composite in air was much higher than that in hydrogen atmosphere, indicating the additional proton conduction in reducing condition. Moreover, the electrolyte resistance reduced when the cell was operated under a current bias compared with the OCV condition. The electrolyte resistance is thought to keep constant or increase in the single ion conductive solid-state ionic conductor, such as YSZ and SDC. Therefore, they proposed that the presence of proton conduction under the current bias condition lead to a higher ionic conductivity and subsequently a lower ohmic resistance compared with that at OCV condition.

DC conductive behaviors of ceria–carbonate composite were also investigated by many researchers [58,60,61,108]. The Sm<sup>3+</sup> and Nd<sup>3+</sup> co-doped ceria and 20 wt% of binary carbonates (Li<sub>2</sub>CO<sub>3</sub>–Na<sub>2</sub>CO<sub>3</sub>) composite gave a DC oxygen conductivity of 0.01 S cm<sup>-1</sup> at 481 °C in air, which is 5 times higher than that of the SDC single-phase material [108]. Besides, the best DC conductivity is obtained at composite with carbonate content of 20 wt%. The authors then suggested that high mobile ion concentration and long jump distance at the interface between SNDC and (Li/Na)<sub>2</sub>CO<sub>3</sub> may contribute to the high conductivity. The electrical conductivity of SDC–Na<sub>2</sub>CO<sub>3</sub> nanocomposite were also studied by Wang et al. [58] using the “four-probe technique” in hydrogen and oxygen atmospheres, respectively. They showed that both proton and oxygen ion transported in the SDC–Na<sub>2</sub>CO<sub>3</sub> nanocomposite; and the proton conductivity is 1–2 orders of magnitude higher than that of the oxygen ionic conductivity in the entire testing temperature range. Besides, they found that the oxygen ionic migration activation energy in the nanocomposite is very close to the single-phase SDC electrolyte while the proton transport activation energy above 350 °C is only 0.272 eV, much lower than proton bulk conductivity in single-phase proton conductor. Hence, they proposed that the oxygen ion migrated in the SDC crystal phase while the proton transfer along the interface of the SDC and Na<sub>2</sub>CO<sub>3</sub> [87]. A similar approach is also employed by Zhao et al. [60] called electrochemical pumping method on the SDC–(Li/Na)<sub>2</sub>CO<sub>3</sub> composite. They found that the composite material showed efficient conductivities of both proton and oxygen ion at 650 °C and the oxygen ionic conductivity surpassed the proton conductivity. While a recent work by Fan and Zhang [61] showed that the proton conduction in SDC–(Li/Na)<sub>2</sub>CO<sub>3</sub> was higher than that of oxygen ion conduction. And the detailed ionic transport/polarization process was discussed based on the intrinsic and extrinsic properties of the proton and oxygen ionic conduction. The multi-ionic conductive property and specific ionic contribution to the total ionic conductivity are uncovered in the DC conductivity measurement. However, it may not reveal the real

condition where both the oxygen ionic and proton as well as the carbonate ion co-transfer in the composite. The results reported depend very much on case to case individual conditions.

Recently, a careful work done by Zhao et al. [59] showed that both the proton and oxygen ions were transported in the composite electrolyte by production analysis and the current interruption technique. When the composite is set in H<sub>2</sub>/O<sub>2</sub> atmosphere, both the oxygen ion and proton conductivities increase with the volume of carbonate in composite. They also found that the presence of CO<sub>2</sub> raised the total ionic conductivity (CO<sub>3</sub><sup>2-</sup>, O<sup>2-</sup> and H<sup>+</sup>). The O<sup>2-</sup> and H<sup>+</sup> conductivities decrease while the conduction of carbonate becomes dominant. Indeed, CO<sub>3</sub><sup>2-</sup> migration is accomplished with the assistance of O<sup>2-</sup>. Thus, the existing of CO<sub>2</sub> in fact improves the oxygen ionic conductivity in fuel cell condition.

As seen from the above discussion, the multi-ionic conduction in the ceria-based composite electrolyte contributes to the total high ionic conductivity, while the contributions of different charge carriers do not follow the same trend, even leading to some contrary results. It should be noticed that the contributions of different ions to the total conductivity in composite electrolyte materials are multi-parameters results, i.e. the electrolyte composition, the microstructures, particle size & distribution and morphology, applied temperature and most importantly the situated gas atmospheres co-determine the final ionic conductivity. Therefore, considerable works are still needed since it would be a very important fundamental issue to understand the ceria–carbonate composite and for future material design for advanced applications, the latter will be discussed in Section 3.3. In addition, the possible multi-ion synergistic or competitive effect is also an interesting topic in this field. More attention may be addressed by the future research.

### 3.2. The ionic conduction mechanisms

The ionic conduction mechanism is always an essential fundamental subject. From the above discussion, we know that the ceria–salt based composites are the mixed ionic conductors: oxygen ion, proton and/or carbonate ion. The ceria is the host of the oxygen ion conducting phase; the transport of the carbonate ion in the molten carbonate composite at certain high temperatures is also easily understood. But, i) how is the extrinsic nature [113] of proton transport in the ceria-salt composite? It is obviously different situation for protons which do not exist originally in the material. Though proton can transport with the carbonate by the chemical intermediate-HCO<sub>3</sub>, it, in some case, dominates the whole conductivity and provides a considerable fuel cell performance [53,58,61]; ii) why does the MCFCs (molten carbonate fuel cells) with a similar electrolyte system show a much lower performance? iii) How is the dual ionic transport process for the oxygen and proton in one composite materials? Will they meet and produce water inside the composite? And so on. Therefore, the study of the ionic conduction behavior and process in the ceria based composite is very interesting but a challenging.

It is well recognized that the conductivity of the polycrystalline materials has been limited by the structural factor – large grain boundary resistance due to the space-charge layer effect as well as the impurity aggregation. The traditional vacancy mechanism can not explain the enhanced ion conductivity anymore. A theoretical calculation gave by Zhu [151] shows that the migration activation energy of the oxygen ionic conduction using the Coulombic model is 0.2 eV based on the interfacial conduction path while it is 1.0 eV for bulk mechanism. Hence, Zhu et al. [43,45,77,151] initially proposed an interfacial conduction mechanism to explain the enhanced oxygen ionic conduction in the ceria-based composites as shown in Fig. 11a. The high concentration oxygen ions/defects on ceria particles surface and interactions with two-phase constitutes

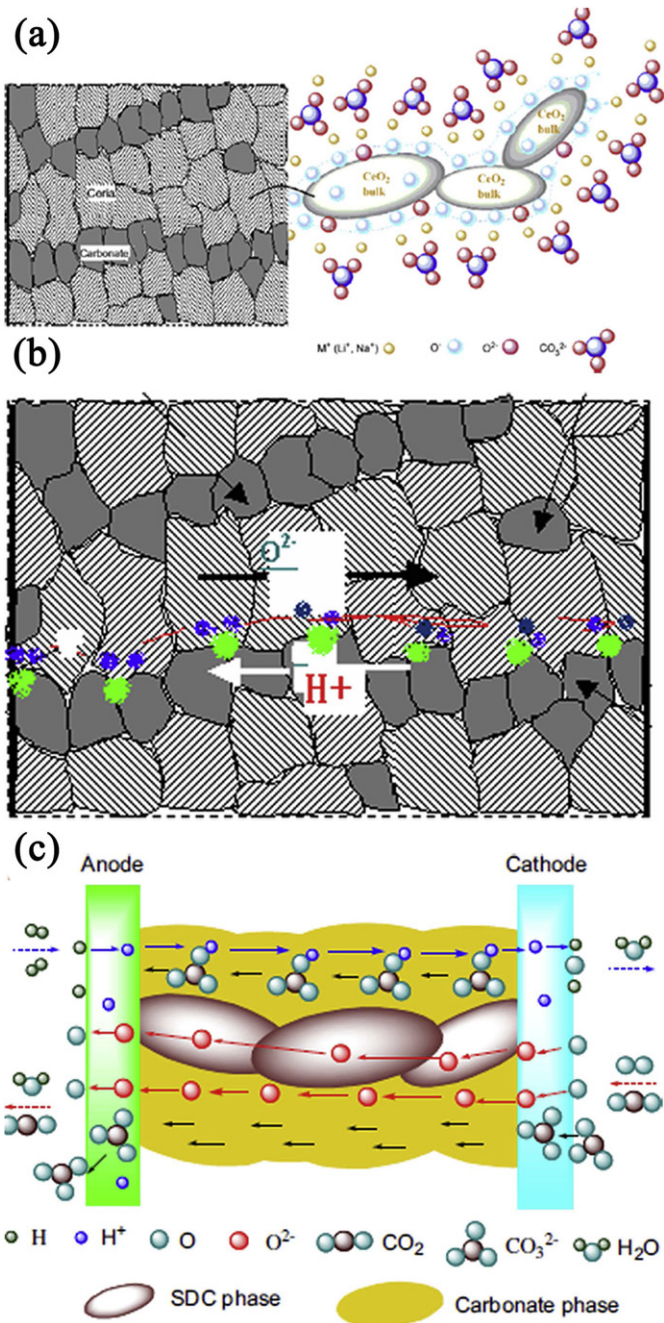


**Fig. 11.** Proposed theoretical interfacial conduction mechanisms (a) for oxygen ionic [151] and (b) for the mixed oxygen ion and proton [45,77] and (c) ionic conduction pathway for oxygen ions, proton and carbonate ions when the cathode gas is the  $O_2$  and  $CO_2$  mixture [59]. Reproduced with permission from Copyright 2008 Elsevier and 2006 Wiley.

may essentially contain ionically conductive highways for proton and oxygen ions in the ceria–carbonate composite materials.

Considering the dual oxygen ion and proton conduction in the ceria-based composite electrolyte as proved by many researchers, Fig. 11b gives an interfacial conducting model [53,58,61]. This model is based on the premise of composite effect: oxygen ion and proton are transported in the individual phases of the composite electrolyte. A conducting chain:  $H\cdots O-H$ ,  $H-O-H$  and  $O-H\cdots O$  atoms/ions exists at the interface of ceria and carbonate. During the transport process, the proton is temporally captured and released by oxygen atoms/ions so that a highway is formed for

proton migration jumping or transferring among oxygens. This may explain the large percentage of proton conduction and impressive high ionic conductivity in the ceria–carbonate composite electrolyte.

A recent theoretical description by Yin et al. [152] revealed that the conductivity of composite electrolytes is linearly increased with the specific SDC–carbonate interface area, which is well agreed with the experimental data obtained by carefully controlling of the contact area between SDC and carbonate using a novel molten salt infiltration technique. The results give an indirect evidence for interfacial ionic conduction in the ceria–carbonate composite electrolyte.

Fig. 11c illustrates an ionic transport scheme for tri-oxygen ion, proton and carbonate ion conduction in the ceria–carbonate composite when the hydrogen as fuel and  $O_2/CO_2$  as the oxidant, which is proposed by Zhao et al. from Tianjin university, China [59]. The hydrogen and oxygen molecules dissociate at the electrode/electrolyte interfaces, and then pass through the bulk electrolyte with the driving force of the potential difference between two electrodes. The carbonate in the electrolyte facilitates the transfer of both ions through hopping. The effect of the  $CO_2$  on the total ionic conductivity and the respective proton and oxygen ion conductivities are carefully analyzed. However, the origin of the enhanced ionic conductivity compared to the conventional SDC electrolyte is not explained. A "Swing Model" has been proposed as a possible mechanism of superior proton conduction in SDC– $Na_2CO_3$  nanocomposite system [58]. This model is still rooted on the interfacial conducting model. The hydrogen bond formed between the  $Ce-O\cdots H\cdots O-CO_2^{2-}$  is thought to provide the high-speed way for proton transport and the presence of the carbonate is vital for this effect. The enhanced bending, stretching vibration of C–O bonds and the promoted mobility and rotation of  $CO_3^{2-}$  group above a critical temperature make the proton transporting easily along a long-range proton transport path under the electrical field. However, this model does not cover other ceria-based composites with a comparable proton and oxygen ionic conductive contributions and in some cases,  $O^{2-}$  can play even a dominant role [56]. Up-to-date, the study of the ionic transport mechanism in a composite electrolyte is still progressing; the electrochemical properties and applications investigations move much faster. While the composite effect or interfacial ionic conduction, which never happens in the bulk materials, may provide novel approaches to achieve unique properties in the composites. The research on the interfacial behavior may lead to explore more functional materials for various energy and environmental applications.

### 3.3. Advanced applications

One of the major research purposes for the nanocomposite materials is to improve higher ionic conductivity for fuel cell application; and it is a truth example for the ceria-based composite electrolytes' excellent electrochemical performances. The recent research on the multi-ionic conducting behaviors of the ceria-salt composites also suggests the possible different applications as shown in the scheme of Fig. 12. Like the conventional SOFC, this novel electrolyte can also be used in electrolysis mode [77,153], the reverse mode of the FC. Using the solid-state matters such as the carbon or lignin as fuel leads to the direct carbon/lignin fuel cell (DCFC) [99,154,155]. The proton conduction in the ceria–salt composite is employed in the ammonia synthesis process [156,157] with less pressure requirement,  $H_2S$  conversion and sulfur capture [82,158,159]. Especially, the carbonate ion transport in the composites suggests a membrane candidate for  $CO_2$  separation [139,160,161], which is a highlighted topic all over the world.

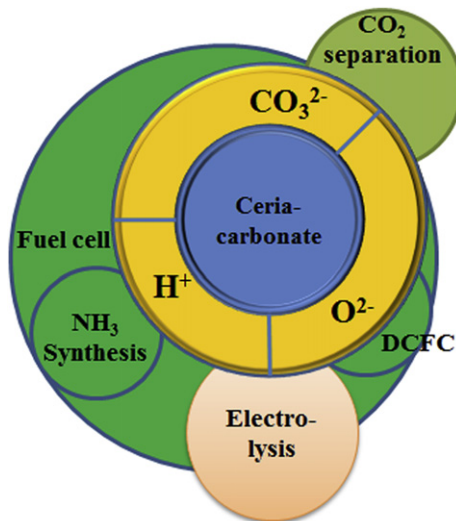


**Fig. 12.** Multi-ionic conduction behaviors and advanced applications of ceria–carbonate composite electrolytes.

### 3.3.1. Electrolysis cell for hydrogen production

Producing hydrogen is a hot topic. Normally, the hydrogen is obtained by the stream reforming of fossil fuel. However, the rapid consumption and depletion of these nonrenewable energy sources provoke scientists to find the sustainable way or to improve the current process energy efficiency. High temperature electrolysis is such a green process with advantages of high efficiency from both thermodynamic and kinetic perspectives, effective approach for large-scale and high-purity hydrogen production [162,163]. In addition, some renewable sources, such as solar and wind energy, can be adopted in this process [164].

Solid oxide electrolysis cell (SOEC) is a reverse process of SOFC. It means that we can produce the hydrogen and oxygen using this technology from water by inputting the electricity as the energy. The feasibility of doped ceria–carbonate nanocomposite electrolyte in the electrolysis is proved by Zhu et al. [153] using Pt paste electrode in 2006. High current output was obtained from the given voltage, suggesting a high hydrogen production rate according to the Faraday law. More importantly, the composite showed that both  $H^+$  and  $O^{2-}$  transport were significant in the composite electrolyte, again proving the mixed ionic conduction properties. More works are required to develop suitable electrode materials replacing Pt to enhance the electrolysis efficiency and reduce the cost of the system as well as to improve the cell operational stability.

### 3.3.2. Direct carbon fuel cell

DCFC is famous for its high theoretical efficiency ( $\geq 100\%$ ) and abundance of solid-state energy sources like wood, biomass that are easily converted to carbon or directly oxidized to obtain the electricity without the combustion process. With the conventional single-phase electrolyte, the limited contact/interface between the carbon and electrolyte, which even gradually reduce with the time, causes large electrode polarization resistance. The use of doped ceria–salt composite could ease this problem to some extent. The molten state or soften state of salts at the elevated temperature can supply more contact areas and then improve the cell performance [99,154]. The high oxygen ionic conductivity promotes the reaction of carbon fuel. Jia et al. [99] reported DCFC based on doped ceria–carbonate with carbon and electrolyte as the anode on the silver Ag current collector. A high performance of  $100 \text{ mW cm}^{-2}$  can be achieved at  $700^\circ\text{C}$  with mixed  $\text{CO}_2/\text{O}_2$  cathode gas, making the DCFC with composite electrolyte a promising device for direct energy conversion.

### 3.3.3. Electrochemical synthesis of ammonia

The proton transport, one of unique characteristics in the doped ceria–carbonate composite, had been employed for electrochemical ammonia synthesis. An ammonia formation rate of  $5.39 \times 10^{-9} \text{ mol s}^{-1} \text{ cm}^{-2}$  was achieved at  $450^\circ\text{C}$  and  $0.8 \text{ V}$  used a cobalt-free  $\text{La}_{0.6}\text{Sr}_{0.4}\text{Fe}_{0.8}\text{Cu}_{0.2}\text{O}_{3-\delta}-\text{Ce}_{0.8}\text{Sm}_{0.2}\text{O}_{2-\delta}$  composite cathode, Ni–SDC anode and SDC– $(\text{Li}/\text{Na}/\text{K})\text{CO}_3$  composite electrolyte with the  $\text{H}_2$  gas in anode chamber and  $\text{N}_2$  in the cathode chamber [51]. The reaction was taken place under the atmospheric pressure, while high pressure of 150–300 bar was needed in the industrial process. In addition, the fast remove of the converted ammonia in  $\text{N}_2$  can solve the limitation of thermodynamic requirements in the conventional process [165]. Furthermore, stable performance was observed during half hour testing. These demonstrated the feasibility of ammonia synthesis through electrochemical process with ceria–carbonate composite ionic conductor. More works are needed to develop high active electrode materials to enhance the reaction kinetics.

### 3.3.4. $\text{CO}_2$ separation

$\text{CO}_2$  capture and storage is a worldwide concerned topic since the discovery of the greenhouse gas effect. To achieve this goal, the  $\text{CO}_2$  should be separated from the other mixed gas. However, the previous processes need the co-transport oxygen and carbonate ions across the membrane plus the external electromotive force. This makes it impossible to separate carbon dioxide and oxygen, simultaneously. It has been proven by Xia et al. [55] that the carbonate ion conduction could be significant in the ceria–carbonate composite. A double ion conduction mechanism that oxygen ions transport in bulk of ceria oxide and carbonate ions pass through in the molten carbonate is proposed in their later work [98]. The double ionic conduction does not need the external oxygen concomitant transport anymore. Therefore, such kinds of membranes provide high selectivity for  $\text{CO}_2$  over other species.

Wade and his coworkers [139,160] studied the  $\text{CO}_2$  selectively separation properties of GDC–carbonate composite material prepared by infiltration method above  $600^\circ\text{C}$ . The flux of  $\text{CO}_2$  across these membranes has reached permeability of  $10^{-11} \text{ mol m}^{-2} \text{ s}^{-1} \text{ Pa}^{-1}$  at  $850^\circ\text{C}$ . In addition, the use of doped ceria oxide with carbonate showed much higher  $\text{CO}_2$  permeability and selectivity compared with the  $\text{Al}_2\text{O}_3$ –carbonates composite, suggesting a synergistic dual-ion transport mechanism. Zhang et al. [161] also found that the highly and efficiently interconnected three-dimensional ionic channels in ceria–carbonate composite by infiltration method offered a high  $\text{CO}_2$  flux density, two orders of magnitude higher than other similar systems reported in the literature. Such an excellent performance points out the great promise of ceria–carbonate composite for selective  $\text{CO}_2$  separation.

Except these advanced applications, the ceria-based composite holds prospect for more other fields, such as the chemicals and electricity co-produce, high valuable solid sulfur recycle and utilization [82].

In addition, there are amount of hints of the multi-ion conduction synergistic effects in the ceria-based composite. However, direct evidences are needed to clarify this issue; the research of the synergistic effect is in the initial stage. More attention is encouraged to reveal to this novel property and its further applications [61].

## 4. Electrode materials research

In previous research, major attentions are focused on the electrical properties study of the composite electrolyte, while the investigations of the electrode materials are very few. It is well known that the electrode materials contribute major polarization

loss for low temperature SOFC and they are actually a limiting factor for further operational temperature reduction of SOFCs, especially from the cathode side [6,166]. Electrode materials possessed excellent compatibility with the ceria-composite electrolyte materials are thus urgently requested. There is a serious situation that the current electrode materials have been developed for intermediate to high temperature SOFC, none of them works properly for the ceria-based composite electrolyte based CFCs. Moreover, the common used cathode materials-lithiated NiO in ceria-based composite electrolyte based CFCs, transferred from the molten carbonate fuel cells (MCFC), has also met similar problem as in MCFC-dissolution in molten carbonate in fuel cell condition. This may lead to electrode/electrolyte interfacial microstructure change and subsequently performance degradation [100,167]. The long-term operation may also cause the short-circuit issue due to the reduction of the dissolved NiO in the composite electrolyte though this problem may be minimized due to the less molten carbonate content used and solid-like core–shell structure constituents. Therefore, the research of suitable electrode materials for low temperature ceria-based composite electrolyte based CFCs possesses tremendous challenges.

#### 4.1. Anode

For CFCs with ceria-based composite electrolyte, the Ni-based cermet electrode is still the state of art anode because it still exhibits adequate catalytic activity toward the hydrogen oxidation reaction at this temperature range [127,173,174]. Some works have attempted to enhance the Ni catalytic activity [126,127,129,131,133,134,174], the major research trend is to develop new anode materials for non-hydrogen fuel utilization, such as methanol, ethanol, biogas, bio-alcohol and Glycerol. The using of non-hydrogen fuel will also promote the commercial visibility of this promising field. Various electrode materials, like metal alloy, transition metal oxide (lithiated or free), CeO<sub>2</sub> and carbon composited metal electrodes are attempted as candidates for different fuels. Summaries of these activities are shown in Table 2. Huang et al. [75] has tried Ni-based double-element alloy (Ni–Fe, Ni–Zn and Ni–Sn) for ethanol fueled ceria-carbonate based CFCs, a OCV of 0.83 V and a maximum power density of 383 mW cm<sup>-2</sup> are achieved at 600 °C. Higher performance of 603 mW cm<sup>-2</sup> has been obtained by Gao [134,169] using ternary Ni–Cu–Zn tri-alloy anode catalyst and methanol as fuel. The lithiated transition metal oxides are also excellent anode candidates for hydrocarbon fueled low temperature CFCs with ceria-based composite electrolyte

[42,75,119,123,140,168,169,170–172]. For example, Imran et al. [172] reported that the lithiated Ni–Cu–Zn oxide gave a peak power density of 584 mW cm<sup>-2</sup> at 570 °C with bio-ethanol as fuel. More importantly, the study of the lithiated transition metal oxide has induced the symmetrical cell and the single-component/electrolyte free fuel cell (SC-EFFC) breakthrough research. The former will be introduced in the following section, while SC-EFFC work will be in the last part of this review.

#### 4.2. Cathode

As mentioned above, the cathode polarization loss will dominate the total polarization below 600 °C, and the additional dissolution of NiO in the molten carbonate will also degrade the fuel cell performance. Therefore, the development of super performance cathode materials has therefore drawn much attention in the past several years. The cathode materials for ceria–carbonate composite electrolyte based SOFC can be typically classified into noble metal materials, mixed ionic/electronic conductive perovskite materials and their composites, and lithiated or lithium free transition metal oxides and their composites [121]. The electrochemical performance of ceria-based composite electrolyte based SOFC with different cathode materials are shown in Table 3.

Noble metals like Pt and Ag are firstly used due to their high oxygen reduction activity, high oxygen dissolution and mobility capability and high electronic conductivity [183]. In the early study, they are used as the cathode for ceria-based double phase electrolyte based SOFC. Hu et al. [83] reported that the Ag electrode with ceria–NaOH composite electrolyte offered a OCV of 1.254 V and a peak output of 716.2 mW cm<sup>-2</sup> at 590 °C with an electrolyte thickness of 0.8–1.2 mm. Zhu et al. also used the Pt as the symmetrical electrode in SOFC to study the H<sub>2</sub>O electrolysis behaviors in the ceria–carbonate composite electrolyte [153]. These noble metals show high electro-catalytic activity, but have been unfavorable maintained for the economic issues.

The perovskite oxides have been widely used in the intermediate/high temperature (600–1000 °C) SOFC because of its high mixed ionic and electronic conductivity and high catalytic activity for oxygen reduction at these temperature ranges. Some of them are naturally grafted to ceria-based composite electrolyte to improve performance and gain sufficient system stability. Ca<sub>0.9</sub>La<sub>0.1</sub>MnO<sub>3</sub> perovskite was first introduced by Kiros et al. [180] in 2001 and achieved a maximum power density of 100–500 mW cm<sup>-2</sup> between

**Table 2**  
Electrochemical performances with ceria–carbonate electrolyte fed with hydrocarbon fuels.

Author	Anode catalyst	Temp. (°C)	Fuel	OCV	P <sub>max</sub> (mW cm <sup>-2</sup> )	Refs.
Zhu	Ni–Cu	600	Methanol	0.91	330	[42]
		600–800	Ethanol	0.87	300	
Huang	Ni–Zn	600	Biomass gas	0.6–0.8	100–700	[168]
	Ni–Sn		Ethanol	0.83	353	[75]
	Ni–Fe			0.93	306	
Gao	LiNiO	512	Methanol	0.78	223	
	Ni–Cu–Zn	600		0.88	550	[140]
		500		0.85	603	[169]
Raza	LiCuNiZnO	550	Bio-gas	0.81	431	
			Bio-methanol bio-ethanol	0.77	300	[170]
				0.94	600	
				0.99	550	
Qin	Li <sub>0.2</sub> Ni <sub>0.7</sub> Cu <sub>0.1</sub> O	580	Glycerol	0.91	215	[171]
			Bio-ethanol	0.81	148	
Imran	LiCuNiZnO	570	Bio-ethanol	–	584	[172]
Mat	Zn–Ni–Cu	580	Alcohol	0.87	500	[121]
Feng	C–MO–CeO <sub>2</sub>	560	Methanol	1.1	250	[119]
Xu	C–(Ni, Cu, Co)O	550	Methanol/3%H <sub>2</sub> O	1.0	258	[123]

**Table 3**

Electrochemical outputs of ceria-based composite electrolyte based SOFCs with different cathodes.

Author	Cathode catalyst	Temp. (°C)	$P_{\max}$ (mW cm <sup>-2</sup> )	Refs.
Zhu B.	LiNiO <sub>2</sub>	400–650	300–800	[43]
Wang X.	LiNiO <sub>2</sub>	550	800	[48]
Hu J.	Ag	590	716.2	[83]
Zhang L.	Sm <sub>0.5</sub> Sr <sub>0.5</sub> Fe <sub>0.8</sub> Cu <sub>0.2</sub> O <sub>3-δ</sub>	525–600	250–370	[92]
Huang J.	La <sub>2</sub> Ni <sub>0.8</sub> Co <sub>0.2</sub> O <sub>4+δ</sub>	500–600	401–700	[113]
Li X.	La(Ni, Fe, Cu)O <sub>3</sub>	450	227	[120, 175–178]
Sun X.	Ba <sub>0.8</sub> Sr <sub>0.2</sub> Co <sub>0.5</sub> –Fe <sub>0.5</sub> O <sub>3-δ</sub>	500	860	[122]
Gao Z.	La <sub>1-x</sub> Sr <sub>x</sub> Ni <sub>y</sub> Fe <sub>1-y</sub> O <sub>3-δ</sub>	600	725	[135]
	SrTi <sub>x</sub> Co <sub>1-x</sub> O <sub>3-δ</sub>		613	[137]
Sun J.	La <sub>2</sub> Ni <sub>1-x</sub> M <sub>x</sub> O <sub>4</sub>	550	312	[179]
Kiros Y.	Ca <sub>0.9</sub> La <sub>0.1</sub> MnO <sub>3</sub> +Ag	450–600	100–500	[180]
Zha. S	La <sub>0.6</sub> Sr <sub>0.4</sub> CoO <sub>3</sub>	530	300	[181]
Fan L.	Pr <sub>2</sub> NiO <sub>4</sub> +Ag	600	695	[125]
Zhu B.	La <sub>0.6</sub> Sr <sub>0.4</sub> Co <sub>0.8</sub> Fe <sub>0.2</sub> O <sub>3</sub>	400–600	200–700	[42,80]
Jing Y.	Li–Ni–Cu–Zn oxide	470	1000	[182]
Zhao Y.		550	730	[128]
Raza R.	NiO/ZnO	500	1107	[126]
Fan L.	Lithiated NiO/ZnO	600	808	[130]

450 °C and 600 °C. The addition of Ag active catalyst into this perovskite promoted the fuel cell performance. A series of LaNi<sub>1-x-y</sub>Fe<sub>x</sub>Cu<sub>y</sub>O<sub>3</sub> oxides was synthesized by Li and his colleagues [120,175–178] and used as the cathode for ceria–carbonate based SOFC to improve the catalytic activity. These materials were carefully prepared with nano-particulate. A maximum power density over 200 mW cm<sup>-2</sup> was obtained at 400 °C. Other perovskite oxides like Sm<sub>0.5</sub>Sr<sub>0.5</sub>Fe<sub>0.8</sub>Cu<sub>0.2</sub>O<sub>3-δ</sub> [92], La<sub>2</sub>Ni<sub>1-x</sub>M<sub>x</sub>O<sub>4</sub> (M = Ni, Fe, Co and Cu) [136,179], Ba<sub>0.8</sub>Sr<sub>0.2</sub>Co<sub>0.5</sub>–Fe<sub>0.5</sub>O<sub>3-δ</sub> [122], La<sub>1-x</sub>Sr<sub>x</sub>Ni<sub>y</sub>Fe<sub>1-y</sub>O<sub>3-δ</sub> [135], SrTi<sub>x</sub>Co<sub>1-x</sub>O<sub>3-δ</sub> [137], La<sub>0.6</sub>Sr<sub>0.4</sub>Co<sub>0.2</sub>Fe<sub>0.8</sub>O<sub>3</sub> (LSCF), La<sub>0.6</sub>Sr<sub>0.4</sub>CoO<sub>3</sub> (LSC) [181], Pr<sub>2</sub>NiO<sub>4</sub>+Ag [125], La<sub>0.6</sub>Sr<sub>0.4</sub>Co<sub>0.8</sub>Fe<sub>0.2</sub>O (LSCF) [42,80] were also attempted. It is worth pointing out here that ceria–carbonate composite electrolyte based SOFC with Sm<sub>0.5</sub>Sr<sub>0.5</sub>Fe<sub>0.8</sub>–Cu<sub>0.2</sub>O<sub>3-δ</sub> cathode showed a very stable performance under 100 h constant/non-stop current density as shown in Fig. 13, while the lithiated NiO cathode exhibited performance degradation in 2 h measurement [92,100]. Therefore, the application of perovskite oxide to replace the lithiated NiO is a possible solution to improve the system durability. Nevertheless, as can be seen from Table 3, the performances of SOFC with perovskite oxides are much

lower than that of lithiated NiO cathode. One possible reason of inferior performance is that their mixed electronic/oxygen ionic conductive property, is not well matched with the mixed proton and oxygen ion conduction behaviors of the ceria-based composite electrolyte in the fuel cell condition. Especially, the proton conductivity may contribute major part of the total conductivity. Therefore, cathode materials with mixed oxygen ionic, proton and electronic conductivity are desirable. Another major reason is the inadequate electro-catalytic function at lower operational temperatures, below 600 °C. In order to improve the performance of perovskite at the reduced the temperatures, Fan et al. [125] developed perovskite oxides compositing with active metal catalyst. It was found that 10 wt% of infiltrated Ag not only reduced the charge transfer resistance but also enhanced the surface catalytic activity of Pr<sub>2</sub>NiO<sub>4</sub>, leading to electrochemical performance enhancement to some extent.

Recently, a series of lithiated transition metal (Ni, Cu, Zn, Fe and Co etc.) oxide (nano) composite was developed by Zhu et al. [79,121,126,128,130,131] with promising catalytic activity for ORR and chemical compatibility with ceria-based composite. These oxide composites maintain the high catalytic activity of lithiated NiO, and simultaneously the doping or compositing of other oxide can effectively reduce the dissolution of NiO in the molten carbonate. Suitable lithiation significantly improves the conductivity of the composite electrode. More importantly, these composites showed multi-functionalities: symmetrical electrode materials for low temperature CFCs and one component device for SC/EFFC device. The partial reduction of metal oxide in the anode atmosphere leads to high *n*-type conduction. The metal alloy may also help to reduce the electrode polarization resistance. Also, existence of the oxide can help to disperse the active metal homogeneously without aggregation. SDC–Na<sub>2</sub>CO<sub>3</sub> electrolyte based SOFC with the lithiated Ni–Cu–Zn oxide as the symmetrical electrode material displayed a maximum power density of 730 mW cm<sup>-2</sup> at 500 °C [128]. More recently, Raza [126] reported that a simple NiO/ZnO symmetrical nanocomposite electrode by facile solid-state reaction presented a peak power density of 1107 mW cm<sup>-2</sup> at 500 °C, which is the ever highest value reported so far. The outstanding performance is attributed to the high electrical conductivity caused by the mutual doping between ZnO and NiO and a dual catalytic functionality both for the anodic fuel oxidation and the cathode oxygen reduction reactions. The mixed *p* and *n*-type conduction in these composite also call forth a breakthrough research – SC/EFFC, see the last section.

Layer lithiated transition metal oxides have realized excellent fuel cell performance and expected high durability. However, few studies have revealed the cathode catalytic losses in this novel system. An investigation by Fan et al. [130] discovered that the lithiated NiO/ZnO performed not so well in air by electrochemical impedance spectroscopy (EIS) measurement in a symmetrical cell configuration; The large polarization resistance should seriously limit the performance of the cell. In addition, they found that the cathode catalytic loss is comparable with the anode catalytic loss and the total electrode polarization resistance is less than 0.3 Ω cm<sup>2</sup>, which meets the high performance cell requirements recommended by Steele B. [138]. The authors thought that the layer transition metal oxides delivered some proton conduction under fuel cell condition [184] and the hydrogen intercalation also improve the material conductivity [185]. The presence of proton conduction in these transition metal oxides may extend the reaction area from the TPB (a site that electrolyte, electrode and porosity meet) to all the internal surface of the electrode, leading to the enhanced performance. More evidences are required to identify these opinions. In addition, the oxygen reduction mechanism on such novel composite system should also be deeply studied

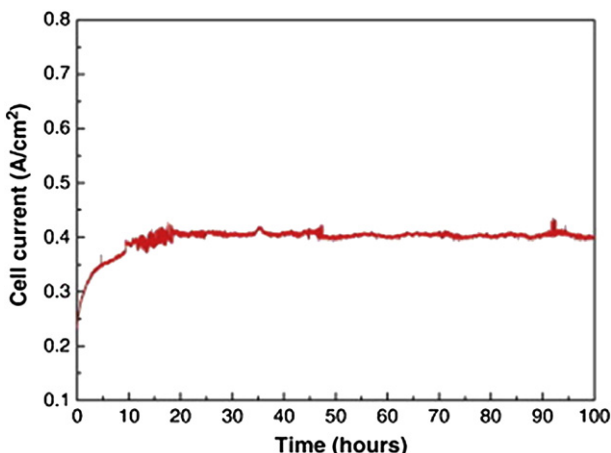


Fig. 13. 100 h ceria–carbonate composite electrolyte based single cell durability test at 550 °C under 0.7 V constant voltage with Sm<sub>0.5</sub>Sr<sub>0.5</sub>Fe<sub>0.8</sub>Cu<sub>0.2</sub>O<sub>3-δ</sub> cathode catalyst [92]. With permission from Elsevier.

considering the high potential of the existing lithiated transition metal oxide electrode and development of novel material systems for super-performance low temperature CFCs as well as the dissimilar working condition compared with the conventional single-phase electrolyte based SOFCs.

## 5. Stability concerning

As a promising electrolyte for CFCs, it should meet several requirements: high ionic conductivity while no electronic conductivity; chemical and thermal stability in fuel cell condition; chemical compatibility with other cell components, like anode and cathode; stable ionic conductivity for long-time operation. The ceria-based composite has satisfied the high ionic conductivity and negligible electronic conductivity for low temperature targeted applications. While in recent years, there are concernings on the nanoparticle/sub-micrometric ceria-oxide grains stability, the carbonate vaporization and decomposition [107], the ionic conductivity stabilization, the chemical compatibility with commonly used electrode materials and long-term fuel cell operation durability issues.

### 5.1. Materials thermal/chemical stability

Benamira et al. [109] had made a systematic investigation of on the thermal, structural and morphological analysis on the GDC based composite materials. They found that these composites kept weight stable after thermal cycling at the temperature range of room temperature to 700 °C and an aging treatment of 168 h at 500 °C. Ma [68] also reported that no weight loss happened from 400 °C to 800 °C in air, suggesting that no volatilization or decomposition reaction occurs on the SDC–Na<sub>2</sub>CO<sub>3</sub> nanocomposite below 800 °C. This may be due to the typical core–shell structure for such nanocomposite material system.

The stability of nano-particle or micrometric ceria oxide grains is a major concern for high temperature operation since the growth of large particulates will reduce the interface area between ceria oxide and carbonate, leading to low conductivity and low catalytic function. By adding a second phase, the grains' growth has been effectively overcome as shown in Fig. 14. The nanoparticle has been clearly distinguished and maintained after annealing at 700 °C for 24 h, while the pure SDC nanoparticle severely agglomerated only after heat-treating at 700 °C for 2 h. So the composite electrolytes show clear thermal stability advantage compared with the single-phase oxide electrolyte. This is extremely important at nano-scale.

The chemical compatibility with other cell components needs also the attention. In the previous section, the dissolution of nickel from the cathode materials into the molten carbonate in the composite leading to the electrolyte/cathode interfacial

microstructure change and performance degradation has been mentioned; this has already been reported by Zhang in their recent work [100]. Therefore, the development novel cathode is a very urgent issue. Some work has been done on this by employing perovskite oxide as cathode, which has proved as a promising strategy to improve the cell operational durability. As shown in Fig. 13, a 100 h stability performance was achieved for CFCs with ceria–carbonate composite electrolyte and Sm<sub>0.5</sub>Sr<sub>0.5</sub>Fe<sub>0.8</sub>Cu<sub>0.2</sub>O<sub>3-δ</sub> cathode, which deserves further effort to improve the cell performance to meet demand for the practical application.

### 5.2. Electrochemical stability

Although there are many reports on conductivity of ceria-based composite, there is little information regarding the behavior of conductivity change against time. The ionic conductivity characteristics are examined using EIS measurements from two groups [90,102,109,186]. Zhang L. [100] tested the conductivity durability of SDC–(Li/Na)<sub>2</sub>CO<sub>3</sub> (carbonate content of 40 wt%) in air. This composite showed unstable ionic conductivity during 2 h measurement. This might be caused by the erosion of carbonate with time and the solid oxide matrix cannot locate the large content of carbonate with proper interfacial configuration in the composite. While Li et al. [102] revealed that the ionic conductivity of ceria–carbonate composite kept constant during 3 days testing period. Longer time conductivity test up to 6000 h has been performed by Benamira [90] as shown in Fig. 15a. A high AC conductivity above 0.07 S cm<sup>-1</sup> has been achieved during the long term stability test, suggesting a great opportunity as the electrolyte material for the practical application.

The stability of ceria based composite electrolyte in fuel cell condition was also extensively investigated. Zhu B. [44] first tested the performance of SDC–20 wt% carbonate up to 4.5 months at 550 °C with hydrogen as fuel and air as the oxidant as shown in Fig. 15b. He found that the maximum power density enhanced with the increase of working time up to 3 months, then reduced in the 4.5 months, indicating a good stability in fuel cell condition. The performance degradation with time after 3 month may relate with the Ni dissolution as well as the carbonate stability with hydrogen gas. Huang et al. [96] also tested the durability of ceria–carbonate composite based SOFC up to 36 h, no obvious degradation phenomenon was observed. In addition, they suggested that adding CO<sub>2</sub> gas to cathode gas would maintain the phase and content stability of carbonate in the composite electrolyte. Following this suggestion, an excellent steady performance was achieved by Li et al. [187] using ceria–carbonate composite electrolyte under simulative MCFC gas atmosphere, i.e. 80% H<sub>2</sub>/20% CO<sub>2</sub> as fuel, and 15% O<sub>2</sub>/30% CO<sub>2</sub>/55% N<sub>2</sub> as oxidant during 200 h testing. Obviously, a fuel cell's long-term stability subjects too many factors except the

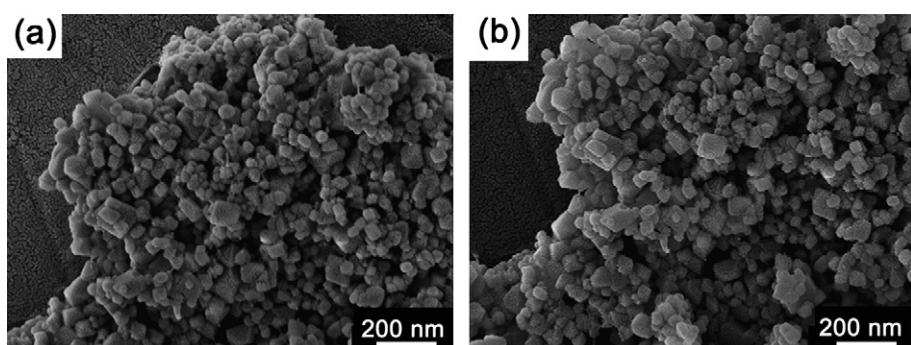
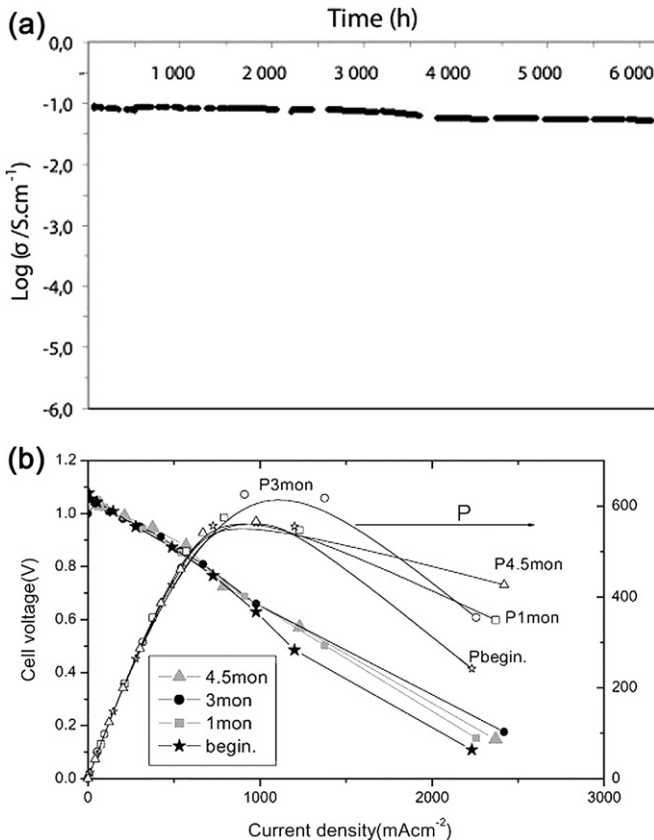


Fig. 14. Stability of SDC–Na<sub>2</sub>CO<sub>3</sub> nanocomposite (a) before and (b) after annealed at 700 °C for 24 h [68].



**Fig. 15.** (a) Time dependence of electrical conductivity of GDC–(Li/K)<sub>2</sub>CO<sub>3</sub> composite at 600 °C in air under OCV condition [90] and (b) evolution of cell performances vs. time for ceria–carbonate composite electrolyte based SOFC at 550 °C [44]. With permission from Elsevier.

above aspects; some other factors, like the microstructure stability of the composite electrolyte and the electrodes as well as the stability of current collector and sealants and so on, should also be clarified. In spite of this, the recent progress on the understanding and experimental measurements has demonstrated a promise of the ceria-based composite electrolyte for high efficient and stable power generations.

## 6. Single-component/electrolyte-free fuel cell based on the nanocomposite materials

Previous sections focus on the composite electrolytes and the compatible electrodes as well as the multi-ionic conduction features for low temperature CFCs or SOFCs and other applications. In this section, a breakthrough research – single-component/electrolyte-free fuel cell (SC-EFFC) [188–198], a joining electrochemical and physical device is presented. This novel device is originated from the above nanocomposite electrolyte and electrode materials and innovative cell configuration research based on NANOCOFC (nanocomposite for advanced fuel cell technology, an EC FP6 project and research network, [www.nanocofc.com](http://www.nanocofc.com)). The electrode materials used in the three-component fuel cells are the mixture of the catalyst, e.g. transition metal oxide and the ionic conducting ceria based composite electrolyte. It was first discovered that the pure electrode materials showed some cell open circuit voltage at tens to hundred mV level when applied by H<sub>2</sub>/air and delivered more than 100 mA current in the same time. With carefully composition optimization between the electronic and ion conducting materials, an OCV above 1.0 V in the H<sub>2</sub>/air condition

and a comparable power output as three-component fuel cells were achieved with the same thickness [189,191,195]. In other words, using these materials could separate the electronic conduction in the anode and cathode to avoid the device short circuit problem without the electron insulating layer-electrolyte. A schematic illustration for three-layer fuel cell and EFFC is shown in Fig. 16a and b, respectively. In the conventional fuel cell (three layer, Fig. 16a), the key components are the anode, electrolyte and cathode, in which electrolyte is indispensable for an electrochemical device to realize the fuel cell function. The ion can pass through the electrolyte while the electron goes from the external circuit from the anode to the cathode. Whereas, in the SC-EFFC (Fig. 16b), the electrolyte layer has been physically removed with only one layer of analogous electrode materials as in the conventional fuel cells. It is amazing to see that this novel structure cell does not show short-circuit problem. Instead, they exhibit similar performance as the conventional SOFC, see Fig. 16c. OCV around 1.0 V and power density of 600 mW cm<sup>-2</sup> were obtained at 550 °C and 300 mW cm<sup>-2</sup> at 450 °C [190].

As mentioned above, the materials in the SC-EFFC are the above described electrode materials for common three-component fuel cells. They are nanocomposite lithiated transition metal oxides with mixed ionic and electronic conductive (MIEC) properties. The crystal structure and morphology of the applied nanocomposite material are shown in Fig. 17. The XRD pattern (Fig. 17a) shows a composite of SDC phase and other metal oxide phases, like NiO, LiFeO<sub>2</sub>, CuO and ZnO. In which the SDC provides the ionic conduction and the metal oxide for electron/hole conduction. The SEM image (Fig. 17b) shows that the average particle size is 100 nm with a narrow distribution. The large particle belongs to the metal oxide due to lower temperature the easy sintering properties effect compared to that of the ceria and the small one is the SDC–carbonate ionic conductor.

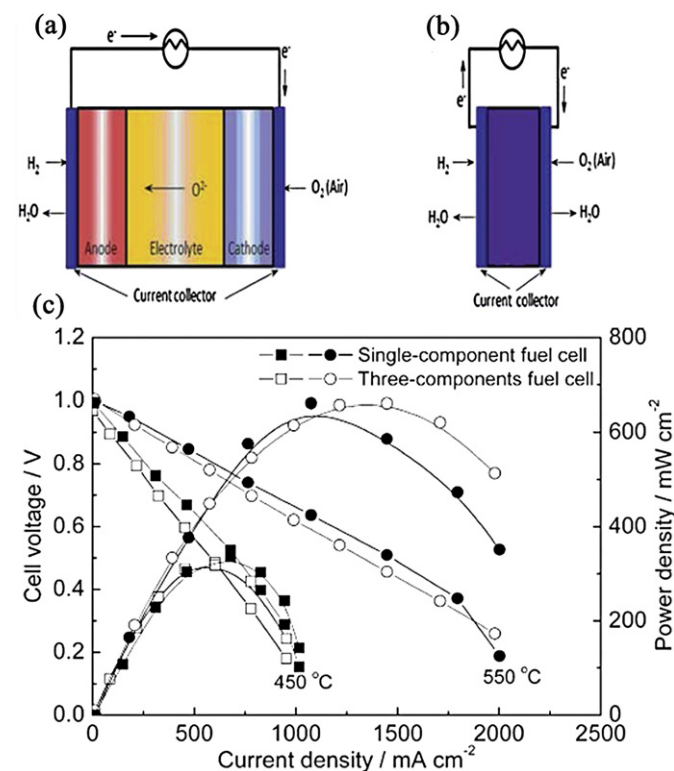


**Fig. 16.** (a, b) Flowchart and (c)  $I$ – $V$  and  $I$ – $P$  characteristics of traditional SOFC and Novel EFFC, respectively [190,193]. Reproduced by permission of The Royal Society of Chemistry and Copyright 2012 Elsevier B.V.

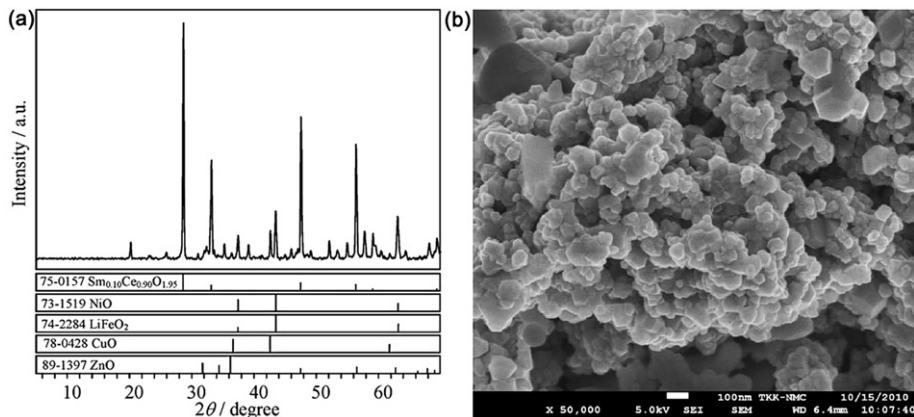


Fig. 17. The crystal structure (a) and microstructure (b) of nanocomposite powder [192]. With permission from Elsevier.

How can the EFFC realize a charge separation while avoid electronic short-circuiting problems? Is there any possible to cause the gas inter-diffusions (hydrogen and the air) using such a porous structure composite? Up to date, the physical principle is still not well understood, the preliminary results showed that SC-EFFC displayed some similarities to solar cells, where semiconductors are used to build the *p–n* junction leading to the electron and hole separation without internal short circuit [199]. For SC-EFFC, different transition metal oxides are used to act as the electro-catalysts for hydrogen oxidation and oxygen reduction reactions. In the same time, the NiO, CuO and LiFeO<sub>x</sub> are the *p*-type semiconductors and ZnO is the *n*-type conductor [192,193,200,201]. The *p*-type conduction can be largely improved by the lithiation reaction or doping/intercalation. In addition, the partial reduction of the transition metal oxide in reduced atmosphere also causes some *n*-type conduction. Therefore, both the *n* and *p* type semiconductors are attributed to the high OCV close to the fuel cell value calculated by the Nernst equation. An *I–V* measurement of this nanocomposite material showed that the current increased significantly when the applied bias voltage is higher than 1.1 V, clearly suggesting the semiconducting properties. While for the reverse mode, the resistance was out of range of the multi-meter, it showed a one-direction current blocking behavior, similar to a diode effect. The possible electrochemical and physical principle (a joint fuel cell and solar cell working principle) is shown in Fig. 18. The electric field is built as soon as the H<sub>2</sub>/Air gases are supplied to

the respective sides due to the bi-catalysis function of this single component nanocomposite. The electric field drives the charge (electrons and holes) separation to form the *p–n* junction barrier and thus the corresponding OCV value. As can be seen from Fig. 18, the holes and electrons move to the corresponding collect collectors, while the ions pass through the bulk of nanocomposite component to realize the fuel cell function.

One may doubt that the gas separation of fuel and oxidant in EFFC will reduce the fuel efficiency and possible gas explosion leading to safety issue. This is a reasonable concern since this device is made by the nanocomposite component with a characteristic of high content of porosity (around 30%). However, according to veser [202], the mixed gas even with a H<sub>2</sub>/O<sub>2</sub> mixture will not react or burn to produce explosion because of the kinetic quenching of the radical chain mechanism in the sub-millimeter porosity range. Besides, a recent theoretical calculation by Q. Liu et al. [197] showed that the reaction depth of hydrogen oxidation and oxygen reduction is in the range of 5.3–1.0 × 10<sup>–2</sup> and 1.4–0.25 × 10<sup>–2</sup> mm at a current density of 100–2000 mA cm<sup>–2</sup> (pellet porosity of 0.5). Both depths are much lower than the typical thickness of the SC-EFFC (0.5 mm). Hence, there is no risk of the explosion under the operating condition for an EFFC and the efficiency is not significantly influenced in this novel energy conversion device.

EFFC device shows many super properties compared with the conventional three layered FC devices. For example, (i) streamlined design with decreased materials, fabrication and operational costs and low requirement of materials compatibility; (ii) better catalyst functions for both electrode reactions; (iii) faster kinetic processes because of the removal of electrode/electrolyte interfaces; (iv) better electrochemical performance due to the reduction of the interface polarization resistance and (v) faster electrochemical response processes due to onsite reactions. From these aspects, we anticipate that EFFC will contribute to considerably simpler and more cost-effective fuel cell construction and system design to accelerate fuel cell commercialization. In addition, the study of SC/EFFC will enrich the fundamental research and understanding of new phenomena in fuel cell science and technology. The discoveries of EFFC maximize the research and knowledge from the previous NANOCOFC R&D. It deserves more extensive development on a simple but multifunctional material component by integrating ionic and semi-conductors/conduction and *p–n* bulk heterojunction and band gap properties as well as catalysts for energy conversion technology and the corresponding cross-linking scientific research. Based on the single component device construction and new scientific principles, it may also provide various possibilities to integrate different energy devices, such as fuel cell, solar

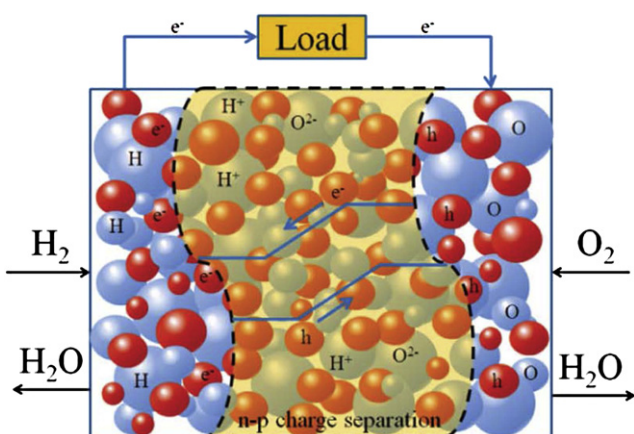


Fig. 18. A joining electrochemical and physical principles of EFFC in hydrogen/air condition [196]. Adapted by permission from The Royal Society of Chemistry.

cells, electrolysis, photo-catalysis and micro-reactors for future sustainable energy conversion and environmental application.

## 7. Summary

Development of ceria-based (nano)composite materials with significantly improved ionic conductivity and electrode catalytic activity based on nanocomposite concept and the interface mechanism are reviewed in this paper. Low temperature ceramic fuel cells with these composite electrolytes show excellent performances. The tunable ionic conduction behaviors (proton, oxygen ion and carbonate) are also attracting a great deal of attention and has been for other advanced applications, such as water electrolysis to H<sub>2</sub> production, DCFC, CO<sub>2</sub> separation and NH<sub>3</sub> atmospheric pressure synthesis. Perovskite oxides provide a prospective solution to improve the durability of composite electrolyte based ceramic fuel cells, while lithiated transition metal oxide nanocomposites are expected to improve the electrochemical performance as well as maintain the system stability. Materials' designing based on the interfacial improvement and functional application also lead to breakthrough research-single component/electrolyte free fuel cell. The simplified materials, fabrication and operation as well as other outstanding characteristics may lead to a new research era on the energy conversion technology from both the commercial and fundamental aspects.

While great progress in the understanding of the hybrid ionic conduction of ceria-based composites and excellent fuel cell performances has been achieved, the detailed conduction mechanism is still unclear. More works are deserved to seek promising all-oxide composite electrolytes at low temperatures, which is still at the early stage. The SC-EFFC based on the single component nanocomposite materials presents an alternative innovation technology for energy conversion, but the cognition of the physical principle is slower than the technical developments. There still has a long-way to go to realize the finally wide implementation of these advanced fuel cell technologies. However, both of them provide possible solutions to conquer the challenges that the conventional high temperature fuel cells meet now.

## Acknowledgments

The Swedish Research Council (VR, No. 621-2011-4983), the Swedish VINNOVA (the Swedish Agency for Innovation) Systems, European Commission FP7 TriSOFc project (No. 303454), KIC Innoenergy and Chinese Scholarship Council (CSC, No. 2010625060), the National Basic Research Program of China (No. 2012CB720302) and the Natural Science Foundation of Tianjin City of China (Key program, No. 12JCZDJC27000) are recognized for the financial support.

## References

- [1] W.R. Grove, *Philos. Mag. Ser.* 14 (1839) 127–130.
- [2] D. Brett, A. Atkinson, N. Brandon, S. Skinner, *Chem. Soc. Rev.* 37 (2008) 1568–1578.
- [3] Z.P. Shao, S.M. Haile, *Nature* 431 (2004) 170–173.
- [4] S. de Souza, S.J. Visco, L.C. De Jonghe, *Solid State Ionics* 98 (1997) 57–61.
- [5] S. d. Souza, S.J. Visco, L.C.D. Jonghe, *J. Electrochem. Soc.* 144 (1997) L35–L37.
- [6] R. Doshi, V. Richards, J. Carter, X. Wang, M. Krumpelt, *J. Electrochem. Soc.* 146 (1999) 1273.
- [7] B.C.H. Steele, *Solid State Ionics* 129 (2000) 95–110.
- [8] H. Huang, M. Nakamura, P. Su, R. Fasching, Y. Saito, F.B. Prinz, *J. Electrochem. Soc.* 154 (2007) B20–B24.
- [9] M. Tsuchiya, B.K. Lai, S. Ramanathan, *Nat. Nanotechnol.* 6 (2011) 282–286.
- [10] E. Wachsman, K. Lee, *Science* 334 (2011) 935–939.
- [11] A. Bieberle-Hütter, D. Beckel, A. Infortuna, U.P. Muecke, J.L.M. Rupp, L.J. Gauckler, S. Rey-Mermet, P. Murali, N.R. Bieri, N. Hotz, M.J. Stutz, D. Poulikakos, P. Heeb, P. Müller, A. Bernard, R. Gmür, T. Hocker, *J. Power Sources* 177 (2008) 123–130.
- [12] B.-K. Lai, K. Kerman, S. Ramanathan, *J. Power Sources* 196 (2011) 6299–6304.
- [13] Y. Takagi, B.-K. Lai, K. Kerman, S. Ramanathan, *Energy Environ. Sci.* 4 (2011) 3473–3478.
- [14] P.C. Su, C.C. Chao, J.H. Shim, R. Fasching, F.B. Prinz, *Nano Lett.* 8 (2008) 2289–2292.
- [15] T. Takahashi, T. Esaka, H. Iwahara, *J. Appl. Electrochem.* 7 (1977) 303–308.
- [16] M. Mori, Y. Liu, M. Shuhua, S.I. Hashimoto, K. Takei, *J. Korean Ceram. Soc.* 45 (2008) 760–765.
- [17] M. Lacerda, J.T.S. Irvine, F.P. Glasser, A.R. West, *Nature* 332 (1988) 525–526.
- [18] T. Ishihara, H. Matsuda, Y. Takita, *J. Am. Chem. Soc.* 116 (1994) 3801–3803.
- [19] S. Nakayama, H. Aono, Y. Sadaoka, *Chem. Lett.* 24 (1995) 431–432.
- [20] P. Lacorre, F. Goutenoire, O. Bohnke, R. Retoux, Y. Lallgant, *Nature* 404 (2000) 856–858.
- [21] C. Zuo, S. Zha, M. Liu, M. Hatano, M. Uchiyama, *Adv. Mater.* 18 (2006) 3318–3320.
- [22] L. Yang, S.Z. Wang, K. Blinn, M.F. Liu, Z. Liu, Z. Cheng, M.L. Liu, *Science* 326 (2009) 126–129.
- [23] S.M. Haile, *Acta Mater.* 51 (2003) 5981–6000.
- [24] S.C. Singhal, K. Kendall, *High Temperature Solid Oxide Fuel Cells: Fundamentals, Design, and Applications*, Elsevier Science, 2003.
- [25] P. Huang, A. Horky, A. Petric, *J. Am. Ceram. Soc.* 82 (1999) 2402–2406.
- [26] A. Matraszek, L. Singheiser, D. Kobertz, K. Hilpert, M. Müller, O. Schulz, M. Martin, *Solid State Ionics* 166 (2004) 343–350.
- [27] A.I. Shaula, V.V. Kharton, F.M.B. Marques, *J. Eur. Ceram. Soc.* 24 (2004) 2631–2639.
- [28] A. Atkinson, *Solid State Ionics* 95 (1997) 249–258.
- [29] S.P.S. Badwal, F.T. Ciacchi, J. Drennan, *Solid State Ionics* 121 (1999) 253–262.
- [30] T.H. Etsell, S.N. Flengas, *Chem. Rev.* 70 (1970) 339–376.
- [31] S.Q. Hui, J. Roller, S. Yick, X. Zhang, C. Deces-Petit, Y.S. Xie, R. Maric, D. Ghosh, *J. Power Sources* 172 (2007) 493–502.
- [32] Q.X. Fu, S.W. Zha, W. Zhang, D.K. Peng, G.Y. Meng, B. Zhu, *J. Power Sources* 104 (2002) 73–78.
- [33] T. Schober, H. Ringel, *Ionics* 10 (2004) 391–395.
- [34] T. Schober, *Electrochim. Solid-State Lett.* 8 (2005) A199–A200.
- [35] C.C. Liang, *J. Electrochim. Soc.* 120 (1973) 1289–1292.
- [36] J.-M. Debierre, P. Knauth, G. Albinet, *Appl. Phys. Lett.* 71 (1997) 1335–1337.
- [37] C. Brahim, A. Ringuedé, E. Gourba, M. Cassir, A. Billard, P. Briois, *J. Power Sources* 156 (2006) 45–49.
- [38] Y. Leng, S. Chan, *Electrochim. Solid-State Lett.* 9 (2006) A56.
- [39] A. Tomita, Y. Tachi, T. Hibino, *Electrochim. Solid-State Lett.* 11 (2008) B68–B70.
- [40] J. Garcia-Barriocanal, A. Rivera-Calzada, M. Varela, Z. Sefrioui, E. Iborra, C. Leon, S.J. Pennycook, J. Santamaria, *Science* 321 (2008) 676–680.
- [41] A. Cavallaro, M. Burriel, J. Roqueta, A. Apostolidis, A. Bernardi, A. Tarancón, R. Srinivasan, S.N. Cook, H.L. Fraser, J.A. Kilner, D.W. McComb, J. Santiso, *Solid State Ionics* 181 (2010) 592–601.
- [42] B. Zhu, *J. Power Sources* 93 (2001) 82–86.
- [43] B. Zhu, *J. Power Sources* 114 (2003) 1–9.
- [44] B. Zhu, X. Yang, J. Xu, Z. Zhu, S. Ji, M. Sun, J. Sun, *J. Power Sources* 118 (2003) 47–53.
- [45] B. Zhu, *Int. J. Energy Res.* 30 (2006) 895–903.
- [46] Z. Bin, *J. Nanosci. Nanotechnol.* 11 (2011) 8873–8879.
- [47] X. Wang, Y. Ma, B. Zhu, *Int. J. Hydrogen Energy* 37 (2012) 19417–19425.
- [48] X. Wang, Y. Ma, R. Raza, M. Muhammed, B. Zhu, *Electrochim. Commun.* 10 (2008) 1617–1620.
- [49] R. Raza, X. Wang, Y. Ma, X. Liu, B. Zhu, *Int. J. Hydrogen Energy* 35 (2010) 2684–2688.
- [50] B. Zhu, *Mater. Res. Bull.* 35 (2000) 47–52.
- [51] B. Zhu, X.R. Liu, T. Schober, *Electrochim. Commun.* 6 (2004) 378–383.
- [52] J. Huang, Z. Mao, Z. Liu, C. Wang, *Electrochim. Commun.* 9 (2007) 2601–2605.
- [53] J. Huang, Z. Mao, Z. Liu, C. Wang, *J. Power Sources* 175 (2008) 238–243.
- [54] C. Xia, Y. Li, Y. Tian, Q. Liu, Y. Zhao, L. Jia, Y. Li, *J. Power Sources* 188 (2009) 156–162.
- [55] C. Xia, Y. Li, Y. Tian, Q. Liu, Z. Wang, L. Jia, Y. Zhao, Y. Li, *J. Power Sources* 195 (2010) 3149–3154.
- [56] J. Di, M. Chen, C. Wang, J. Zheng, L. Fan, B. Zhu, *J. Power Sources* 195 (2010) 4695–4699.
- [57] L. Fan, C. Wang, M. Chen, J. Di, J. Zheng, B. Zhu, *Int. J. Hydrogen Energy* 36 (2011) 9987–9993.
- [58] X. Wang, Y. Ma, S. Li, A.-H. Kashyout, B. Zhu, M. Muhammed, *J. Power Sources* 196 (2011) 2754–2758.
- [59] Y. Zhao, C. Xia, Y. Wang, Z. Xu, Y. Li, *Int. J. Hydrogen Energy* 37 (2012) 8556–8561.
- [60] Y. Zhao, C. Xia, Z. Xu, Y. Li, *Int. J. Hydrogen Energy* 37 (2012) 11378–11382.
- [61] L. Fan, G. Zhang, M. Chen, C. Wang, J. Di, B. Zhu, *Int. J. Electrochem. Sci.* 7 (2012) 8420–8435.
- [62] A.S. Arico, P. Bruce, B. Scrosati, J.-M. Tarascon, W. van Schalkwijk, *Nat. Mater.* 4 (2005) 366–377.
- [63] Y. Liu, S. Zha, M. Liu, *Adv. Mater.* 16 (2004) 256–260.
- [64] M.G. Bellino, D.G. Lamas, N.E. Walsöe de Reca, *Adv. Funct. Mater.* 16 (2006) 107–113.
- [65] T. Sholklapper, H. Kurokawa, C. Jacobson, S. Visco, L. De Jonghe, *Nano Lett.* 7 (2007) 2136–2141.
- [66] C.C. Chao, Y.B. Kim, F.B. Prinz, *Nano Lett.* 9 (2009) 3626–3628.

[67] J. Maier, *Nat. Mater.* 4 (2005) 805–815.

[68] Y. Ma, X. Wang, R. Raza, M. Muhammed, B. Zhu, *Int. J. Hydrogen Energy* 35 (2010) 2580–2585.

[69] J. Maier, *Solid State Ionics* 157 (2003) 327–334.

[70] H.L. Tuller, *Solid State Ionics* 131 (2000) 143–157.

[71] S. Kim, J. Maier, *J. Electrochem. Soc.* 149 (2002) J73–J83.

[72] S. Kim, J. Maier, *J. Eur. Ceram. Soc.* 24 (2004) 1919–1923.

[73] W. Zhu, C. Xia, D. Ding, X. Shi, G. Meng, *Mater. Res. Bull.* 41 (2006) 2057–2064.

[74] B. Zhu, *Int. J. Energy Res.* 33 (2009) 1126–1137.

[75] J. Huang, F. Xie, C. Wang, Z. Mao, *Int. J. Hydrogen Energy* 37 (2012) 877–883.

[76] B. Zhu, B. Mellander, *Ionics* 3 (1997) 368–372.

[77] B. Zhu, M.D. Mat, *Int. J. Electrochem. Sci.* 1 (2006) 383–402.

[78] Y. Ma, X. Wang, S. Li, M.S. Toprak, B. Zhu, M. Muhammed, *Adv. Mater.* 22 (2010) 1640–1644.

[79] L. Fan, C. Wang, B. Zhu, *Nano Energy* 1 (2012) 631–639.

[80] B. Zhu, X.R. Liu, P. Zhou, Z.G. Zhu, W. Zhu, S.F. Zhou, *J. Mater. Sci. Lett.* 20 (2001) 591–594.

[81] Q.X. Fu, W. Zhang, R.R. Peng, D.K. Peng, G.Y. Meng, B. Zhu, *Mater. Lett.* 53 (2002) 186–192.

[82] X.R. Liu, B. Zhu, J.R. Xu, J.C. Sun, Z. Mao, *Key Eng. Mater.* 280–283 (2004) 425–430.

[83] J. Hu, S. Tosto, Z. Guo, Y. Wang, *J. Power Sources* 154 (2006) 106–114.

[84] J. Wu, B. Zhu, Y. Mi, S.-J. Shih, J. Wei, Y. Huang, *J. Power Sources* 201 (2012) 164–168.

[85] R. Raza, G. Abbas, X. Wang, Y. Ma, B. Zhu, *Solid State Ionics* 188 (2011) 58–63.

[86] R. Raza, G. Abbas, S.K. Imran, I. Patel, B. Zhu, *J. Fuel Cell. Sci. Technol.* 8 (2011) 041012.

[87] J. Huang, L. Zhang, C. Wang, P. Zhang, *Int. J. Hydrogen Energy* 37 (2012) 13044–13052.

[88] J. Huang, Z. Mao, L. Yang, R. Peng, *Electrochem. Solid-State Lett.* 8 (2005) A437–A440.

[89] J. Huang, Z. Gao, Z. Mao, *Int. J. Hydrogen Energy* 35 (2010) 4270–4275.

[90] M. Benamira, A. Ringuedé, L. Hildebrandt, C. Lagergren, R.N. Vannier, M. Cassir, *Int. J. Hydrogen Energy* 37 (2012) 19371–19379.

[91] R. Chockalingam, S. Basu, *Int. J. Hydrogen Energy* 36 (2011) 14977–14983.

[92] L. Zhang, R. Lan, A. Kraft, S. Tao, *Electrochem. Commun.* 13 (2011) 582–585.

[93] L. Zhang, R. Lan, X. Xu, S. Tao, Y. Jiang, A. Kraft, *J. Power Sources* 194 (2009) 967–971.

[94] S.A. Song, S.-C. Jang, J. Han, S.P. Yoon, S.W. Nam, I.-H. Oh, T.-H. Lim, *J. Power Sources* 196 (2011) 9900–9905.

[95] C.M. Lapa, F.M.L. Figueiredo, D.P.F. de Souza, L. Song, B. Zhu, F.M.B. Marques, *Int. J. Hydrogen Energy* 35 (2010) 2953–2957.

[96] J. Huang, L. Yang, R. Gao, Z. Mao, C. Wang, *Electrochem. Commun.* 8 (2006) 785–789.

[97] Z. Gao, Z. Mao, C. Wang, J. Huang, Z. Liu, *Int. J. Energy Res.* 33 (2009) 1138–1144.

[98] Y. Li, Z. Rui, C. Xia, M. Anderson, Y.S. Lin, *Catal. Today* 148 (2009) 303–309.

[99] L. Jia, Y. Tian, Q. Liu, C. Xia, J. Yu, Z. Wang, Y. Zhao, Y. Li, *J. Power Sources* 195 (2010) 5581–5586.

[100] L. Zhang, R. Lan, C.T.G. Petit, S. Tao, *Int. J. Hydrogen Energy* 35 (2010) 6934–6940.

[101] I.A. Amar, R. Lan, C.T.G. Petit, V. Arrighi, S. Tao, *Solid State Ionics* 182 (2011) 133–138.

[102] X. Li, G. Xiao, K. Huang, *J. Electrochem. Soc.* 158 (2011) B225–B232.

[103] L. Zhang, X. Li, S. Wang, K.G. Romito, K. Huang, *Electrochem. Commun.* 13 (2011) 554–557.

[104] Y. Xia, Y. Bai, X. Wu, D. Zhou, X. Liu, J. Meng, *Int. J. Hydrogen Energy* 36 (2011) 6840–6850.

[105] M. Mizuhata, Y. Harada, G.-j. Cha, A.B. Beleke, S. Deki, *J. Electrochem. Soc.* 151 (2004) E179–E185.

[106] A. Bodén, J. Di, C. Lagergren, G. Lindbergh, C.Y. Wang, *J. Power Sources* 172 (2007) 520–529.

[107] V. Jain, S. Bobade, D. Gulwade, P. Gopalan, *Ionics* 16 (2010) 487–496.

[108] W. Liu, Y.Y. Liu, B. Li, T.D. Sparks, X. Wei, W. Pan, *Compos. Sci. Technol.* 70 (2010) 181–185.

[109] M. Benamira, A. Ringuedé, V. Albin, R.N. Vannier, L. Hildebrandt, C. Lagergren, M. Cassir, *J. Power Sources* 196 (2011) 5546–5554.

[110] T. Cai, Y. Zeng, S. Yin, L. Wang, C. Li, *Mater. Lett.* 65 (2011) 2751–2754.

[111] M. Cassir, S.J. McPhail, A. Moreno, *Int. J. Hydrogen Energy* 37 (2012) 19345–19350.

[112] A.S.V. Ferreira, T. Saradha, F.L. Figueiredo, F.M.B. Marques, *Int. J. Energy Res.* 35 (2011) 1090–1099.

[113] A.S.V. Ferreira, C.M.C. Soares, F.M.H.L.R. Figueiredo, F.M.B. Marques, *Int. J. Hydrogen Energy* 36 (2011) 3704–3711.

[114] S. Muhammed Ali, A. Muchtar, N. Muhamad, A.B. Sulong, in: 2011 IEEE First Conference on Clean Energy and Technology CET Print (2011), ISBN 978-1-4577-1353-8, pp. 394–399.

[115] T. Ristoiu, T. Petrisor Jr., M. Gabor, S. Rada, F. Popa, L. Ciontea, T. Petrisor, *J. Alloys Compd.* 532 (2012) 109–113.

[116] T. Saradha, A.S. Ferreira, S.G. Patrício, F.M.L. Figueiredo, F.M.B. Marques, *Int. J. Hydrogen Energy* 37 (2012) 7235–7241.

[117] M. Mizuhata, T. Ohashi, A.B. Béléké, *Int. J. Hydrogen Energy* 37 (2012) 19407–19416.

[118] B. Zhu, B.E. Mellander, *Solid State Ionics* 70–71 (1994) 285–290.

[119] B. Feng, C.Y. Wang, B. Zhu, *Electrochem. Solid-State Lett.* 9 (2006) A80–A81.

[120] S. Li, J.C. Sun, X.L. Sun, B. Zhu, *Electrochem. Solid-State Lett.* 9 (2006) A86–A87.

[121] M. Mat, X. Liu, Z. Zhu, B. Zhu, *Int. J. Hydrogen Energy* 32 (2007) 796–801.

[122] X.L. Sun, S. Li, J.C. Sun, X.R. Liu, B. Zhu, *Int. J. Electrochem. Sci.* 2 (2007) 462–468.

[123] S. Xu, X. Niu, M. Chen, C. Wang, B. Zhu, *J. Power Sources* 165 (2007) 82–86.

[124] B. Zhu, X.R. Liu, Y. Cheng, M.L. Zhang, *Key Eng. Mater.* 336–338 (2007) 428–433.

[125] L. Fan, M. Chen, C. Wang, B. Zhu, *Int. J. Hydrogen Energy* 37 (2012) 19388–19394.

[126] R. Raza, Q. Liu, J. Nisar, X. Wang, Y. Ma, B. Zhu, *Electrochem. Commun.* 13 (2011) 917–920.

[127] R. Raza, B. Zhu, T.H. Fransson, *J. Fuel Cell. Sci. Technol.* 8 (2011) 031010.

[128] Y. Zhao, D.-B. Xiong, H. Qin, F. Gao, H. Inui, B. Zhu, *Int. J. Hydrogen Energy* 37 (2012) 19351–19356.

[129] G. Abbas, M.A. Chaudhry, R. Raza, M. Singh, Q. Liu, H. Qin, B. Zhu, *Nanosci. Nanotechnol. Lett.* 4 (2012) 389–393.

[130] L. Fan, B. Zhu, M. Chen, C. Wang, R. Raza, H. Qin, X. Wang, X. Wang, Y. Ma, *J. Power Sources* 203 (2012) 65–71.

[131] W. Tan, L. Fan, R. Raza, M. Ajmal Khan, B. Zhu, *Int. J. Hydrogen Energy* 38 (2013) 370–376.

[132] R. Raza, G. Abbas, Q. Liu, I. Pate, B. Zhu, *J. Nanosci. Nanotechnol.* 12 (2012) 4994–4997.

[133] C. Zhou, J. Huang, P. Zhang, Z. Gao, Z. Mao, *Acta Energ. Sol. Sin.* 30 (2009) 985–989.

[134] Z. Gao, Z. Mao, C. Wang, Z. Liu, *Int. J. Hydrogen Energy* 35 (2010) 12897–12904.

[135] Z. Gao, Z. Mao, C. Wang, Z. Liu, *Int. J. Hydrogen Energy* 35 (2010) 12905–12910.

[136] J. Huang, R. Gao, Z. Mao, J. Feng, *Int. J. Hydrogen Energy* 35 (2010) 2657–2662.

[137] Z. Gao, Z. Mao, C. Wang, Z. Liu, *Int. J. Hydrogen Energy* 36 (2011) 7229–7233.

[138] B.C.H. Steele, *Solid State Ionics* 86–88 (1996) 1223–1234.

[139] J.L. Wade, C. Lee, A.C. West, K.S. Lackner, *J. Membr. Sci.* 369 (2011) 20–29.

[140] Z. Gao, R. Raza, B. Zhu, Z. Mao, C. Wang, Z. Liu, *Int. J. Hydrogen Energy* 36 (2011) 3984–3988.

[141] Z. Tang, Q. Lin, B.-E. Mellander, B. Zhu, *Int. J. Hydrogen Energy* 35 (2010) 2970–2975.

[142] L. Fan, C. Wang, J. Di, M. Chen, J. Zheng, B. Zhu, *J. Nanosci. Nanotechnol.* 12 (2012) 4941–4945.

[143] R. Raza, G. Abbas, B. Zhu, Asme, *GDC-Y<sub>2</sub>O<sub>3</sub> Oxide Based Two Phase Nanocomposite Electrolytes*, Amer Soc Mechanical Engineers, New York, 2010.

[144] B. Zhu, *Solid State Ionics* 145 (2001) 371–380.

[145] B. Zhu, G. Lindbergh, D. Simonsson, *Corros. Sci.* 41 (1999) 1497–1513.

[146] W. Jamsak, S. Assabumrungrat, P.L. Douglas, N. Laosiripojana, R. Suwanwarangkul, S. Charojoachkul, E. Croiset, *Chem. Eng. J.* 133 (2007) 187–194.

[147] B. Heed, B. Zhu, B.E. Mellander, A. Lundén, *Solid State Ionics* 46 (1991) 121–125.

[148] M. Dudek, *J. Eur. Ceram. Soc.* 28 (2008) 965–971.

[149] H. Chen, Z. Xu, C. Peng, Z. Shi, J.-L. Luo, A. Sanger, K.T. Chuang, *Ceram. Int.* 36 (2010) 2163–2167.

[150] H. Wang, J. Xiao, Z. Zhou, F. Zhang, H. Zhang, G. Ma, *Solid State Ionics* 181 (2010) 1521–1524.

[151] B. Zhu, S. Li, B.E. Mellander, *Electrochem. Commun.* 10 (2008) 302–305.

[152] S. Yin, Z. Ye, C. Li, X. Chen, Y. Zeng, *Mater. Lett.* 92 (2013) 78–81.

[153] B. Zhu, I. Albinsson, C. Andersson, K. Borsand, M. Nilsson, B.E. Mellander, *Electrochem. Commun.* 8 (2006) 495–498.

[154] M. Chen, C. Wang, X. Niu, S. Zhao, J. Tang, B. Zhu, *Int. J. Hydrogen Energy* 35 (2010) 2732–2736.

[155] H. Li, Q. Liu, Y. Li, *Electrochim. Acta* 55 (2010) 1958–1965.

[156] I. Amar, R. Lan, C. Petit, S. Tao, *J. Solid State Electrochem.* 15 (2011) 1845–1860.

[157] I.A. Amar, C.T.G. Petit, L. Zhang, R. Lan, P.J. Skabar, S. Tao, *Solid State Ionics* 201 (2011) 94–100.

[158] B. Zhu, *Fuel Cells Bull.* 2 (1999) 9–12.

[159] B. Zhu, S. Tao, *Solid State Ionics* 127 (2000) 83–88.

[160] J.L. Wade, A.C. West, K.S. Lackner, *213th ECS Meeting Abstracts*, vol. 1, 2008, p. 390.

[161] L. Zhang, N. Xu, X. Li, S. Wang, K. Huang, W.H. Harris, W.K.S. Chiu, *Energy Environ. Sci.* 5 (2012) 8310–8317.

[162] M. Ni, M.K.H. Leung, D.Y.C. Leung, *Int. J. Hydrogen Energy* 33 (2008) 2337–2354.

[163] A. Brisse, J. Scheffold, M. Zahid, *Int. J. Hydrogen Energy* 33 (2008) 5375–5382.

[164] C.M. Stoops, J.E. O'Brien, K.G. Condie, J.J. Hartvigsen, *Int. J. Hydrogen Energy* 35 (2010) 4861–4870.

[165] G. Marnellos, G. Karagiannakis, S. Zisekas, M. Stoukides, *Stud. Surf. Sci. Catal.* 130 (2000) 413–418.

[166] Y.D. Zhen, A.I.Y. Tok, S.P. Jiang, F.Y.C. Boey, *J. Power Sources* 178 (2008) 69–74.

[167] K. Ota, S. Mitsushima, S. Kato, S. Asano, H. Yoshitake, N. Kamiya, *J. Electrochem. Soc.* 139 (1992) 667–671.

- [168] B. Zhu, X.Y. Bai, G.X. Chen, W.M. Yi, M. Bursell, *Int. J. Energy Res.* 26 (2002) 57–66.
- [169] Z. Gao, R. Raza, B. Zhu, Z. Mao, *Int. J. Energy Res.* 35 (2011) 690–696.
- [170] R. Raza, H. Qin, Q. Liu, M. Samavati, R.B. Lima, B. Zhu, *Adv. Energy Mater.* 1 (2011) 1225–1233.
- [171] H. Qin, Z. Zhu, Q. Liu, Y. Jing, R. Raza, S. Imran, M. Singh, G. Abbas, B. Zhu, *Energy Environ. Sci.* 4 (2011) 1273–1276.
- [172] S. Imran, R. Raza, G. Abbas, B. Zhu, *J. Fuel Cell. Sci. Technol.* 8 (2011) 061014–061016.
- [173] R. Raza, B. Zhu, *J. Nanosci. Nanotechnol.* 11 (2011) 5450–5454.
- [174] R. Raza, X. Wang, Y. Ma, B. Zhu, *J. Power Sources* 195 (2010) 8067–8070.
- [175] S. Li, X. Sun, Z. Wen, J. Sun, *Rare Met.* 25 (2006) 213–217.
- [176] J. Sun, C. Wang, S. Li, S. Ji, *J. Korean Ceram. Soc.* 45 (2008) 755–759.
- [177] C. Wang, X. Sun, S. Li, S. Ji, J. Sun, *Chin. J. Power Sources* 32 (2008) 177–179.
- [178] S. Li, B. Zhu, *J. Nanosci. Nanotechnol.* 9 (2009) 3824–3827.
- [179] J. Sun, S. Li, S. Ji, Z. Wen, *Int. J. Energy Res.* 35 (2011) 1032–1036.
- [180] Y. Kirov, X.R. Liu, B. Zhu, *J. New Mater. Electrochem. Syst.* 4 (2001) 253–258.
- [181] S. Zha, J. Cheng, Q. Fu, G. Meng, *Mater. Chem. Phys.* 77 (2003) 594–597.
- [182] Y. Jing, H. Qin, Q. Liu, M. Singh, B. Zhu, *J. Nanosci. Nanotechnol.* 12 (2012) 5102–5105.
- [183] T. Huang, X. Shen, C. Chou, *J. Power Sources* 187 (2009) 348–355.
- [184] S. Tao, Q. Wu, Z. Zhan, G. Meng, *Solid State Ionics* 124 (1999) 53–59.
- [185] Z. Zhou, K. Kato, T. Komaki, M. Yoshino, H. Yukawa, M. Morinaga, K. Morita, *J. Eur. Ceram. Soc.* 24 (2004) 139–146.
- [186] X. Li, G. Xiao, S.M. Lee, K. Huang, *ECS Trans.* 33 (2011) 87–103.
- [187] S. Li, J. Sun, *Int. J. Hydrogen Energy* 35 (2010) 2980–2985.
- [188] *Nat. Nanotechnol.* 6 (2011) 330.
- [189] B. Zhu, Y. Ma, X. Wang, R. Raza, H. Qin, L. Fan, *Electrochem. Commun.* 13 (2011) 225–227.
- [190] B. Zhu, H. Qin, R. Raza, Q. Liu, L. Fan, J. Patakangas, P. Lund, *Int. J. Hydrogen Energy* 36 (2011) 8536–8541.
- [191] B. Zhu, R. Raza, G. Abbas, M. Singh, *Adv. Funct. Mater.* 21 (2011) 2465–2469.
- [192] B. Zhu, R. Raza, H. Qin, L. Fan, *J. Power Sources* 196 (2011) 6362–6365.
- [193] B. Zhu, R. Raza, H. Qin, Q. Liu, L. Fan, *Energy Environ. Sci.* 4 (2011) 2986–2992.
- [194] H. Qin, B. Zhu, R. Raza, M. Singh, L. Fan, P. Lund, *Int. J. Hydrogen Energy* 37 (2012) 19365–19370.
- [195] L. Fan, C. Wang, O. Osamudiamen, R. Raza, M. Singh, B. Zhu, *J. Power Sources* 217 (2012) 164–169.
- [196] B. Zhu, R. Raza, Q. Liu, H. Qin, Z. Zhu, L. Fan, M. Singh, P. Lund, *RSC Adv.* 2 (2012) 5066–5070.
- [197] Q. Liu, H. Qin, R. Raza, L. Fan, Y. Li, B. Zhu, *RSC Adv.* 2 (2012) 8036–8040.
- [198] Y. Xia, X. Liu, Y. Bai, H. Li, X. Deng, X. Niu, X. Wu, D. Zhou, M. Lv, Z. Wang, J. Meng, *RSC Adv.* 2 (2012) 3828–3834.
- [199] B. O'Regan, M. Gratzel, *Nature* 353 (1991) 737–740.
- [200] W. Shin, N. Murayama, *Mater. Lett.* 45 (2000) 302–306.
- [201] S. Jung, K. Yong, *Chem. Commun.* 47 (2011) 2643–2645.
- [202] G. Veser, *Chem. Eng. Sci.* 56 (2001) 1265–1273.